MODELING THE IMPACT OF IONIC LIQUID ELECTROLYTES ON THE LITHIUM-SULFUR BATTERY PERFORMANCE

by

Şeyda Asarkaya

B.S., Chemical Engineering, Boğaziçi University, 2021

Submitted to the Institute for Graduate Studies in
Science and Engineering in partial fulfillment of
the requirements for the degree of
Master of Science

Graduate Program in Chemical Engineering
Boğaziçi University

2024

ACKNOWLEDGEMENTS

During my master's program, I obtained significant experience, knowledge, and abilities that I could showcase in my personal, academic, and professional pursuits. As a result, this journey turned into an unforgettable experience in my life due to the people who supported me throughout it.

First and foremost, I would like to thank my thesis advisor, Assoc. Prof. Damla Eroğlu Pala, for giving a chance to involve her research gorup. I am truly thankful for her patience, kindness, and the support she provided throughout my thesis research. She is a role model for me, demonstrating exceptional diligence, multitasking skills, and a positive attitude as a mentor.

I am also thankful to my thesis thesis committee members, Prof. Ramazan Yıldırım and Assoc. Prof. Burak Ülgüt, for being in my thesis committee and being supportive and indulgent.

I would also like to thank all faculty members of the Department of Chemical Engineering and the members of the EChemE research group.

I would like to thank my dearest friend Aysun Çeçe for making my university years much more enjoyable. I would also like to thank my lifelong friends Beyza İnce, Elif Kanıboz, Seda Varol, Sena Duman, Cansu Aygün, and Didem Çiçek for being there when I needed their support.

I would like to thank my husband, Uğur Kocabaş, and my brother, Ahmet Asarkaya, for their support, love, and encouragement.

I would like to offer a special thanks to my parents, Nilgün Asarkaya and Vahit Asarkaya, for their unconditional love. Without them, I would never have been the person I am today.

ABSTRACT

MODELING THE IMPACT OF IONIC LIQUID ELECTROLYTES ON THE LITHIUM-SULFUR BATTERY PERFORMANCE

The lithium-sulfur (Li-S) battery is a promising future technology as an energy storage system due to its cost-effectiveness, high theoretical capacity, and energy density. However, fully understanding the complex electrochemical mechanisms remains a significant challenge for further advancement and commercial feasibility. Design parameters of Li-S cells, especially the ones regarding the electrolyte, can significantly impact their performance. In this thesis, a zero-dimensional electrochemical model is established to highlight the impact of electrolyte design parameters. The (Yan, Yin, Guo, & Wan, 2014) (Yan, Yin, Guo, & Wan, 2014) the active reaction area, initial voltage, shuttle and precipitation constants, standard potentials, exchange current densities, C-rate, and the electrolyte-to-sulfur (E/S) ratio is investigated. Simulations were performed using Fortran programming language to illustrate discharge and charge profiles. The impact of the E/S ratio on the discharge and charge profiles is investigated by altering the electrolyte volume in the cell in the model. An increase in the discharge capacity is expected with an increase in the E/S ratio. However, the model is unable to predict this trend. In addition, a sensitivity analysis was performed to see the dependence of the results on the selected model parameters regarding electrolyte design; this way, the impact of ionic liquid electrolyte design on the performance can be captured implicitly. An increase in the exchange current densities causes almost no change in the cell voltage and capacity for all three stages of redox reactions in the model. The changes in discharge and charge profiles are also negligible in terms of the changes in active reaction area and initial voltage parameters. Nevertheless, the influence of the shuttle constant on cell performance is significant; the capacity decreases significantly with increasing the shuttle constant. The model cannot reflect the effect of C-rate as mass transfer is neglected in a zero-dimensional model. In conclusion, a zero-dimensional model is utilized to investigate the impact of electrolyte design parameters through sensitivity analysis. It is successful in predicting the influence of certain parameters. The effect of the electrolyte quantity on battery performance is not observable in the suggested model.

ÖZET

İYONİK SIVI ELEKTROLİTLERİN LİTYUM-KÜKÜRT BATARYA PERFORMANSI ÜZERİNDEKİ ETKİSİNİN MODELLENMESİ

Lityum-kükürt (Li-S) bataryası, maliyet verimliliği, yüksek teorik kapasitesi ve enerji yoğunluğu sayesinde yenilenebilir enerji kaynağı olarak gelecek vaat eden bir teknoloji olarak görülmektedir. Ancak, kompleks elektrokimyasal mekanizmaların tam olarak anlaşılmaması, bu bataryanın gelişimi ve ticari olarak uygulanabilirliği için büyük bir engel oluşturmaktadır. Li-S batarya hücrelerinin tasarım parametreleri, batarya performansını önemli ölçüde etkileyebilir. Bu tezde, hücre tasarım parametrelerinin etkisini vurgulamak için sıfır boyutlu bir elektrokimyasal model oluşturulmuştur. Aktif reaksiyon alanı, başlangıç voltajı, mekik ve çökelme sabitleri, standart potansiyeller, değişim akım yoğunlukları, C oranı ve elektrolit-kükürt (E/S) oranının etkisi incelenmiştir. Fortran programlama dili kullanılarak deşarj ve şarj profillerini göstermek için simülasyonlar yapılmıştır. Model, elektrolit-kükürt oranının deşarj performansına etkisini tahmin etmede başarısız olmuştur. E/S oranı hücredeki elektrolit hacmini değiştirerek ayarlanmıştır. E/S oranının artmasıyla deşarj kapasitesinde bir artış beklenmektedir. Ancak simulasyonlarda gözlemlenmemiştir. Ayrıca, elektrolit tasarım parametreleri ile ilgili bir duyarlılık analizi gerçekleştirilmiştir. Model, kütle transferini içermediği için C oranının etkisini yansıtma konusunda başarısız olmuştur. Değişim akım yoğunluklarındaki artış, tüm redoks reaksiyon aşamaları için hücre voltajında ve kapasitede neredeyse hiçbir değişikliğe yol açmamıştır. Benzer şekilde modelde aktif reaksiyon alanı ve başlangıç voltajdaki değişiklikler deşarj ve şarj profillerinde değişiklik yaratmamıştır. Bununla birlikte, mekik sabitinin hücre performansı üzerindeki etkisi doğru bir şekilde yakalanmıştır; artan mekik sabiti ile kapasite önemli ölçüde azalmaktadır. Sonuç olarak, sıfır boyutlu model, duyarlılık analizi yoluyla elektrolit tasarım parametrelerinin etkisini araştırmak için kullanılmıştır. Belirli parametrelerin etkisini tahmin etmede başarılıdır. Önerilen modelde elektrolit miktarının batarya performansı üzerindeki etkisi gözlemlenmemiştir.

TABLE OF CONTENTS

LIST OF FIGURES

LIST OF TABLES

LIST OF SYMBOLS

a_r	Active reaction area per cell
C_i	Concentration of components, i
E_j	Nernst potentials of electrochemical reaction *j*
E_j^0	Standard potential of electrochemical reaction *j*
F	Faraday's constant
f_H	Dimensionality factor of high electrochemical reaction
f_L	Dimensionality factor of low electrochemical reaction
f_M	Dimensionality factor of medium electrochemical reaction
i_j	Current density of electrochemical reaction j
$i_{j,ref}^0$	Exchange current density of j^{th} electrochemical reaction
i_s	Solid phase current density
I	Current density
k_p	Precipitation rate constant
k_s	Shuttle constant
M_{S_8}	Molar Mass of S_8
n_j	The number of electrons transferred for j^{th} electrochemical reaction
$n_{S_8^0}$	The number of sulfur atoms per molecule
$n_{S_4^{2-}}$	The number of sulfur atoms per molecule
$n_{S_2^{2-}}$	The number of sulfur atoms per molecule
$n_{S^{2-}}$	The number of sulfur atoms per molecule
R	Universal gas constant
t	Time
T	Temperature
V_{cell}	Cell voltage

ρ_S	Density of precipitated Sulfur
η_j	Overpotential of electrochemical reaction j

1. INTRODUCTION

Fossil fuels are mostly used as energy sources to meet energy demand. However, since fossil fuels are one of the major reasons for today's increasing effects of global warming and air pollution, research on alternative energy sources is rising. Renewable energy sources like solar, wind, and waves also need energy storage, whereas geothermal energy is only utilized in specific regions. Rechargeable batteries are seen as promising sources for mobile chemical energy storage [1]. While the trend toward sustainable technologies is increasing, battery technologies have become one of the widely used environmentally friendly systems, with their high energy storage function. From electronic vehicles to medical equipment, its scope of use is expanding. Many countries and plants have begun to make rules or applications and establish a mindset to diminish fossil fuel-based energy consumption in various fields like vehicles [2].

During the 1970s, Li batteries were introduced to the market [3]. Lithium-ion batteries have gained prominence as they offer the highest energy density and efficiency among rechargeable batteries. This has led to extensive research focused on developing new materials and improving the cost, energy output, efficiency, and safety of Li-ion batteries [4]. Current difficulties include expanding their application to high-power and large-scale uses. Li-ion batteries show poor performance at high temperatures and have a limited cycle life due to surface effects on electrodes that raise impedance during cycling. The safety measures of commercially available Li-ion batteries are inadequate for large-scale applications, driving recent research efforts to develop new solvents, salts, and additives to enhance performance [5].

The use of lithium-ion batteries spread to areas such as electronic or medical devices. The maximum discharge capacity of Li-ion batteries is about 250 mAh g^{-1}. However, the maximum discharge capacity lithium-ion batteries can achieve does not fulfill today's energy demand required for various markets [6]. Thus, different types of batteries are developed and continue to be improved as an alternative to Li-ion batteries. Lithium-oxygen ($Li–O_2$) and lithium-sulfur (Li–S) batteries are two major types of batteries of interest to many researchers [7]. When the two are compared, the specific energy density of Li-S

batteries is lower than Li–O_2, yet more research is being done on Li-S batteries. Although both are not commercialized, Li-S batteries are more likely to be used in markets soon [7]. Li-S batteries are the trending topic in the energy field for their theoretically high specific energy and capacity, low cost, and environmentally friendly nature. On the other hand, safety, cost, and higher performance are some problems that still need to be solved [8].

High capacities and enhanced cycle life are the two important sides of Li- S batteries that should be improved. Thus, material designs such as encapsulated cathodes with structured carbons, binder and electrolyte types, and S loading in the cathode are the major research areas in the field. In order to reach the theoretical capacity of 3860 mAh g^{-1} of Li metal, various salts, additives, and electrolyte types that will make an interface between anode and electrolyte are also investigated in the literature [9].

Sulfur shows great potential as a cathode material with a theoretical capacity of 1675 mAh g^{-1}, which is the highest among solid elements besides being one of the most abundant elements in nature. Sulfur has numerous advantages, such as being low cost, unlike other materials used in batteries, and being environmentally friendly. Generally, Li-S cells are composed of a lithium metal anode, an organic liquid electrolyte, and a composite sulfur cathode [10]. During the discharge process, lithium metal undergoes an oxidation reaction at the anode, producing lithium ions and electrons. Lithium ions move toward the positive electrode through the electrolyte, while electrons migrate to the positive electrode through the external electrical circuit, generating an electrical current. At the cathode, lithium ions and electrons are accepted to reduce sulfur into lithium sulfide. The reactions that occur during the discharge are reversed in the charging process [11]. The Figure 1.1 shows the general mechanism of Li-S batteries.

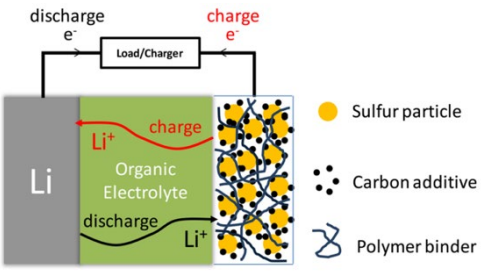

Figure 1.1. Schematic diagram of lithium-sulfur batteries Reprinted (adapted) with permission from [11]. Copyright 2014 American Chemical Society.

At the beginning of discharge, the Li anode undergoes oxidation to form Li^+ ions. These ions move through the electrolyte to the sulfur cathode, where solid sulfur (S_8) accepts the Li^+ ions and an electron, forming soluble Li_2S_8. Later, Li_2S_8 is gradually reduced through multiple electrochemical steps to produce insoluble Li_2S or Li_2S_2. Typical discharge and charge profiles of Li-S batteries can be seen in Figure 1.2.

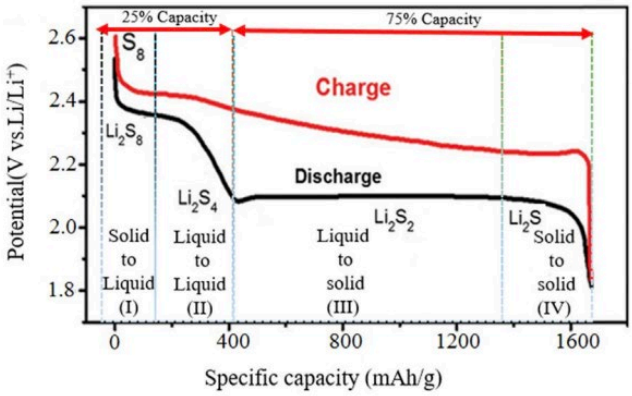

Figure 1.2. Discharge and Charge profile of a Li-S battery [12].

When sulfur is reduced into solid Li_2S or Li_2S_2 through discharge, four-phase transitions are defined as stated in Figure 1.2. The first phase is a two-step reaction from solid elemental sulfur (S_8) to dissolved long-chain lithium polysulfides at approximately 2.4 V and the reaction can be expressed as [12] [13]

$$S_8 + 2Li^+ + 2e^- \rightarrow Li_2S_8. \quad (1.1)$$

In the second phase, Li_2S_8 is further reduced, forming dissolved short-chain lithium polysulfides. This reaction is represented by the liquid-liquid transition can be written as [12] [13]

$$Li_2S_8 + 2Li^+ + 2e^- \rightarrow 2Li_2S_4. \quad (1.2)$$

In the third phase, at approximately 2.1 V, a two-step reaction occurs. Short-chain lithium polysulfides reduced to solid Li_2S or Li_2S_2 can be given as [12] [13]

$$Li_2S_4 + 2Li^4 + 2e^- \rightarrow 2Li_2S_2, \quad (1.3)$$

$$Li_2S_4 + 6Li^+ + 6e^- \rightarrow 4Li_2S. \quad (1.4)$$

In the final phase, reactions to form insoluble and nonconductive solid Li_2S can be expressed as [12] [13]

$$Li_2S_2 + 2Li^+ + 2e^- \rightarrow 2\,Li_2S. \quad (1.5)$$

The dip point seen between phases two and three is due to the increase of viscosity in the electrolyte that hinders Li^+ ion transport. Furthermore, in order to crystallize ionically/electrically insulating Li_2S_2, an overpotential is required. An important amount of the discharge capacity, approximately 75%, arises from phase three and four reactions [13].

One of the main challenges in Li-S batteries to overcome is the dissolution of soluble polysulfides into the electrolyte. During the charge process, solid Li_2S / Li_2S_2 particles are oxidized into long-chain polysulfides. At first, the amount of long-chain polysulfides on the cathode side is low. Thus, electric field force suppresses diffusion gradients. As the charging process continues, an increase in the long-chain polysulfide concentration causes diffusion forces to be stronger than the electric field force. As a result, long-chain polysulfides migrate to and are reduced at the lithium metal anode. The short-chain polysulfides move back to the cathode, and the oxidation process reoccurs. Some of the products of the reactions at the anode undergo a further reduction process, which results in Li_2S / Li_2S_2. These insoluble solid products cover the surface of the lithium anode. This mechanism is called the polysulfide shuttle mechanism. The low current density of charge enhances the shuttle effect [14] [15]. Cell performance is significantly affected by the polysulfide shuttle mechanism. The loss of active sulfur, Li_2S / Li_2S_2 passivation on the lithium anode surface, low utilization of the sulfur cathode, and degradation of cycle life are the main drawbacks [16].

Another critical point that influences cell performance is electrolyte design, both electrolyte type and amount. The volume of the electrolyte strongly influences the sulfur redox reactions. The electrolyte-to-sulfur (E/S) ratio, which is a common metric to quantify the electrolyte volume in the cell, has an essential role in the electrochemical performance and overall energy density of Li-S batteries. Reducing the amount of electrolyte positively affects the energy density [17]. On the other hand, the utilization of the active material increases with higher E/S ratios, leading to an increase in the discharge capacity. Low E/S ratios can hinder electrochemical reactions due to polysulfide solubility limits. Thus, discharge capacity decreases [9]. Moreover, when the E/S ratio is low, an increase in the concentration gradient is observed that aggravates the polysulfide shuttle [17]. On the other hand, the polysulfide shuttle mechanism also enhances at very high E/S ratios.

In literature, there are various studies on electrolyte type, which highly influences cell performance. Electrolyte types can be divided into various categories, such as solid-state electrolytes, polymer electrolytes, liquid, glass-ceramic, and hybrid electrolytes. Key properties desired in electrolytes to enhance cell performance include strong ionic conductivity, electronic insulation, and stability across thermal, mechanical, and electrochemical conditions across a wide potential range. Furthermore, electrolytes should be non-reactive with other battery components, such as separators, electrodes, and casings. Since these requirements can sometimes conflict, electrolyte formulations frequently combine solvents with varied physical and chemical properties to achieve the best overall performance [18]. Low conductivity at room temperature and significant interfacial resistance restrict the kinetic properties in solid-state electrolytes [19]. 1,3-dioxolane (DOL) and 1,2-dimethoxyethane (DME) are widely utilized as ether solvents in lithium-sulfur (Li-S) batteries due to their advantageous properties, including low viscosity, high lithium salt solubility, and satisfactory chemical and electrochemical stability. However, a drawback of these ether solvents is their solvation ability, which can result in the excessive dissolution of polysulfides. Ionic liquids are promising alternatives widely studied for rechargeable lithium-sulfur batteries. Their wide, stable potential range, combined with low volatility and flammability, contributes to improved safety in cells. Additionally, their limited donor ability effectively decreases the solubility of polysulfides [20].

C-rate is another parameter that strongly influences battery performance and cell capacity. At higher current density, discharge capacity decreases because of mass transport limitations [9].

1.1. Aim and Scope of Current Work

Lithium-sulfur batteries are considered as a good energy storage alternative. Nevertheless, numerous challenges need to be resolved for the commercialization of lithium-sulfur batteries, primarily due to their complex electrochemical reaction mechanisms, which remain poorly understood. The problems due to the dissolution, diffusion, and side reactions of soluble lithium polysulfides are the main challenges to overcome as they result in issues such as irreversible loss of active materials, reduced coulombic efficiency, decreased stability, and rapid capacity decline [21].

The electrolyte types used in lithium-sulfur batteries have a significant impact on the cell performance. The aim of this thesis is to develop a model to illustrate the influence of ionic liquid electrolytes on the Li-S cell discharge and charge performance. The effect of electrolyte properties and the electrolyte-to-sulfur (E/S) ratio on the cell performance is evaluated through model parameters. The goal of this research is to identify which model parameters are influenced by the ionic liquid electrolyte properties and the nature of that influence. Chapter 2 includes a comprehensive review of the studies about material design, the effect of electrolyte types, electrolyte amount, design parameters that influence cell performance, and the E/S ratio.

A zero-dimensional mathematical model is proposed based on the article published by Cornish and Marinescu [22]. The model operates at constant current. The redox reactions that occur in the cathode are defined as three-stage reactions with the shuttle effect considered. The Fortran programming language is used. The discharge and charge profiles of lithium-sulfur batteries with ionic liquid electrolytes are simulated. The effect of model parameters and the E/S ratio on the cell performance is investigated through discharge and charge profiles. In Chapter 3, the mathematical model is explained in detail.

In Chapter 4, a sensitivity analysis is performed on the model parameters defined in Chapter 3 in order to evaluate the influence of electrolyte design. The voltage versus capacity profiles of discharge and charge processes are simulated with varying values of the active reaction area, initial cell voltage, shuttle constant, precipitation constant, standard potentials of three redox reactions, exchange current densities, and C-rate. Additionally, the electrochemical performance of the lithium-sulfur battery is investigated in terms of the electrolyte-to-sulfur ratio in the cell. The effect of the E/S ratio is evaluated through the changes in the electrolyte amount. Through these analyses, the impact of electrolyte type is investigated. The results of the simulations and discussion are detailed. In Chapter 5, a comprehensive overview of the study's findings and insights is provided.

2. LITERATURE REVIEW

A summary of earlier research on the effects of electrolyte composition and characteristics on Li-S battery performance is given in this section of the thesis.

The design and type of electrolyte, along with the amount of electrolyte used, affects cell performance. The different types of electrolytes used in the Li-S batteries are mainly classified into four categories: non-aqueous liquids, ionic liquids, solid polymers, and glass-ceramic electrolytes [6]. Various electrolyte types, salts, and additives are used to prevent undesired reactions of lithium with the electrolyte, resulting in changes in the surface structure of the anode [9]. Electrolytes made of ions at room temperature are called room-temperature ionic liquids (RTILs). They are advantageous in many aspects, such as low volatility, nonflammability, and melting point, high thermal stability and ionic conductivity, a broad range of electrochemical potential and others [23].

One of the major problems of the electrolyte is the highly reactive characteristics of polysulfides. Widely used solvents such as esters, carbonates, and phosphates react rapidly with the polysulfides. In electrolytes, DME and DOL solvents can be used as a mixture due to their unique advantages. Although dimethyl ether (DME) solvent has higher solubility of polysulfides compared to 1,3-dioxolane (DOL), it shows more reactivity with the Li metal. For the DOL, the situation is exactly the opposite. Thus, combining both creates a synergetic effect on the performance of the Li-S batteries [24].

Sheng S. Zhang tried to optimize the E/S ratio in the Li-S batteries by evaluating the cycling performance of Li-S cells. 0.25 m $LiSO_3CF_3$-0.25 m $LiNO_3$ dissolved in a 1:1 (wt:wt) mixture of dimethyl ether (DME) and 1,3-dioxolane (DOL) was used as electrolyte in the study. The study found that after 100 cycles at 0.5 mA cm^{-2} between 1.7 V and 2.8 V, a Li/S cell with a 72% sulfur cathode and 2 mg cm−2 sulfur loading may maintain a specific capacity of 780 mAh g^{-1} [25].

Park et al. mentioned that aprotic room-temperature ionic liquids have weak Lewis acidic cations and basic anions. However, typical organic molecular solvents such as THF,

DOL, and DME have strong Lewis basic anions. Additionally, the weak Lewis basic anion lowers the solubility of polysulfides in electrolytes due to their low donor ability. In the research conducted with the binary RTIL (Li [TFSA]/[DEME][TFSA]), lower solubility of polysulfides, high Coulombic efficiency, and longer cycle life are observed [23].

Chen et al. studied lithium trifluoromethyl-4,5-dicyanoimidazole (LiTDI) to investigate the influence of LiTDI on the battery performance and the solubility of polysulfides. The investigation is conducted with a high sulfur loading of 3 mg/cm^2. They show that the LiTDI salt decreases the solubility of polysulfides [26].

Drvarič Talian et al. investigated the effect of lithium ions on battery performance. The electrolyte consists of [DEME][TFSI] ionic liquid,1,3-dioxolane (DOL), and LiTFSI salt with different compositions. They observed that increasing the DOL composition in the electrolyte causes lower Coulombic efficiencies and larger capacity fade. The amount of ionic liquid is directly proportional to the efficiency. However, increasing the ionic liquid amount has drawbacks like higher viscosity and polarization and lower specific capacity [18].

Shın et al. made an examination using N-methyl-(n-butyl)pyrrolidinium bis(trifluoromethanesulfonyl)imide (PYR14TFSI), 0.5 M LiTFSI, poly(ethylene glycol) dimethyl ether (PEGDME) mixture in the electrolyte. It is stated that enhanced charge/discharge cyclability and ionic conductivity are observed by increasing PEGDME in the mixture. The presence of PYR14TFSI also positively affects thermal stability and conductivity. Thus, the ternary mixture is suggested as a promising electrolyte for Li-S batteries [27].

The effects of numerous solvent compositions on cell performance and electrolyte characteristics were examined by Lu Hai et al. Ionic liquid N,N-diethyl-N-methyl-N-(2-methoxyethyl)ammonium bis(trifluoromethyl sulfonyl) amide (DEMETFSI) and individual or binary co-solvent(s) contain 1,1,2,2-tetrafluoroethyl-2,2,3,3-tetrafluoropropyl ether (TTE) and/or 1,3-dioxolane (DOL) were used. It is stated that the hybrid DEMETFSI/TTE/DOL system performed better than the ionic liquid electrolytes with no

co-solvent or with a single co-solvent since TTE and DOL act in conjunction to strengthen ionic conductivity and Li surface chemistry [28].

Peng et al. studied to determine how salt concentration affected the ionic liquid electrolyte's characteristics and the Li–S battery's electrochemical performance through concentrated imidazolium-based ionic liquid electrolytes, getting the benefit of the synergistic advantages of both ionic liquids and high-concentration electrolytes. It has been discovered that increasing the concentration of salt can efficiently inhibit the dissolution of lithium polysulfides due to increased viscosity and a protective layer structure on the cathode, which improves the stability of the Li anode [29].

Recently, Pushpa Selvi et al. investigated the effect of electrolyte additives using triethyl sulfonium bis (trifluoro methane sulfonyl) imide [S222] [TFSI] as an electrolyte additive. The base electrolyte was prepared by combining 1,3-dioxolane (DOL) and tetra ethylene glycol dimethyl ether (TEGDME)1: 1 (v/v) with 1 M of LiTFSI in an argon atmosphere. Then, the electrolyte additive [S222] [TFSI] was mixed with the base electrolyte at a 1:3 volume ratio. According to the results, high ionic conductivity, stable interfacial resistance, and low self-discharge were the properties of the hybrid electrolyte. The electrolyte additive can dissolve short-chain polysulfide deposits on the surface of the cathode. It promotes higher sulfur utilization and minimizes capacity loss [30].

Marinescu et al. developed a zero-dimensional mathematical model to capture the cell performance of Li-S cells during the charge and discharge process. The model assumes two-phase electrochemical reactions during discharge. The shuttle effect and the precipitation of short-chain lithium polysulfides are implicitly taken into consideration in the proposed model with shuttle and precipitation constants. The voltage versus capacity profiles are simulated by changing model parameters to evaluate the effect of the C-rate and the precipitation. Changes in the C-rate are evaluated by considering or neglecting the kinetic limitations and precipitation. The model with kinetic limitations but without precipitation is not sensitive to the C-rate since the discharge profile does not meet the expected behaviours of the experimental data. When the discharge profile is captured with the model, including kinetic limitations and precipitation, for various C-rates, it is observed that higher C-rates lower the dip point between two voltage plateaus. According to the results, when increasing

the C-rate, a higher total discharge capacity is observed. Increasing the precipitation constant enhances the voltage output in the low-voltage plateau. Additionally, increasing the precipitation constant during charge causes slower dissolution, resulting in higher voltage [31].

3. MODEL DEVELOPMENT

The zero-dimensional model proposed by Cornish and Marinescu is applied in this thesis to investigate the effect of ionic liquid electrolytes on the Li-S cell discharge performance [22]. The complicated Li-S cell reaction mechanism observed in experimental studies can be reduced to a less complex mechanism within a zero-dimensional model. For instance, a zero-dimensional model may diminish the number of assumed parameters due to the complexity of higher-dimensional models [22]. Thus, the proposed model in the study is zero-dimensional, and to reduce the complexity of the model, some assumptions are made. The electrochemical reactions are modelled with a three-step mechanism. Additionally, during charge, the electrochemical reactions that happen in discharge are assumed to be reversed. The concentrations of the species do not change with position but with time during discharge and charge. The kinetics are defined according to the Butler-Volmer kinetics, and the charge transfer coefficients for the anodic and cathodic processes are assumed to be equal and are taken as 0.5 [32]. The shuttle effect is also taken into consideration in this model. The model is executed with a constant current charge and constant current discharge, just for the cathode. Also, temperature is assumed to be constant.

The model proposed has three electrochemical reactions occurring during discharge and charge, can be written as

$$S_8^0 + 4e^- \rightarrow 2S_4^{2-}, \tag{3.1}$$

$$S_4^{-2} + 2e^- \rightarrow 2S_2^{2-}, \tag{3.2}$$

$$S_2^{-2} + 2e^- \rightarrow 2S^{2-} \downarrow. \tag{3.3}$$

The first reaction is used to model the high voltage discharge plateau, whereas the second and the third reactions are used to describe the lower voltage plateau. In the following parts, the reactions will be stated as high, medium, and low voltage reactions, respectively. The subscripts written as h, m, and l in the equations correspond to the high, medium, and low voltage reactions mentioned above, respectively.

Butler-Volmer kinetics are used to describe the reaction rates and, thus, the current densities i_H, i_M, and i_L (A m^{-2}) can be written as

$$i_H = -2i_H^0 a_r sinh\frac{n_H F}{2RT}\eta_H, \tag{3.4}$$

$$i_M = -2i_M^0 a_r sinh\frac{n_M F}{2RT}\eta_M, \tag{3.5}$$

$$i_L = -2i_L^0 a_r sinh\frac{n_L F}{2RT}\eta_L. \tag{3.6}$$

Here, a_r (m^{-2}) is the active surface area of the cathode, n_H, n_M, and n_L are the number of electrons transferred for each reaction, and Faraday's constant is symbolized as F in the units of C mol^{-1}. R (J K^{-1} mol^{-1}) is the gas constant, T is the temperature of the reactions in K, n_H, n_M, and n_L are the reaction overpotentials, and i^0_H, i^0_M, and i^0_L (A m^{-2}) are the exchange current densities for the three electrochemical reactions.

The overpotentials (in V) are calculated using Nernst potentials and dilute solution theory, can be shown as

$$\eta_H = V - E_H, \tag{3.7}$$

$$\eta_M = V - E_M, \tag{3.8}$$

$$\eta_L = V - E_L, \tag{3.9}$$

$$E_H = E_H^0 + \frac{RT}{n_H F} l\,n\left(f_H \frac{S_8^0}{(S_4^{2-})^2}\right), \tag{3.10}$$

$$E_M = E_M^0 + \frac{RT}{n_M F} l\,n\left(f_M \frac{S_4^{2-}}{(S_2^{2-})^2}\right), \tag{3.11}$$

$$E_L = E_L^0 + \frac{RT}{n_L F} l\,n\left(f_L \frac{S_2^{2-}}{(S^{2-})^2}\right), \tag{3.12}$$

where V is the cell voltage and E_H, E_M, E_L are the Nernst potentials, both in V. E_H^0, E_M^0, and E_L^0 are the standard potentials in V and f_H, f_M, and f_L are dimensionality constants in g*L* mol^{-1}.

Since the model is zero-dimensional, the mass transfer of species due to diffusion and migration is not considered. The change of species with time due to electrochemical and precipitation/dissolution reactions during discharge can be written as

$$\frac{dS_8^0}{dt} = -\frac{M_S * n_{S_8^0}}{n_H F} i_H - k_S^{(T)} S_8^0, \tag{3.13}$$

$$\frac{dS_4^{2-}}{dt} = \frac{M_S * n_{S_8^0}}{n_H F} i_H + k_S^{(T)} S_8^0 - \frac{M_S * n_{S_4^{2-}}}{n_M F} i_M, \tag{3.14}$$

$$\frac{dS_2^{2-}}{dt} = \frac{M_S * n_{S_4^{2-}}}{n_M F} i_M - \frac{M_S * n_{S_2^{2-}}}{n_M L} i_L, \quad (3.15)$$

$$\frac{dS^{2-}}{dt} = \frac{M_S * n_{S_2^{2-}}}{n_M L} i_L - \frac{k_{p/d}^{(T)}}{\upsilon \rho_s} S_p \left(S^{2-} - S_*^{(T)} \right), \quad (3.16)$$

$$\frac{dS_p}{dt} = \frac{k_{p/d}^{(T)}}{\upsilon \rho_s} S_p \left(S^{2-} - S_*^{(T)} \right), \quad (3.17)$$

where $k_p/d(T)$ is the precipitation/dissolution rate constant in s-1, M_s is the molar mass of sulfur in g mol^{-1}, $k_s(T)$ is the shuttle constant, and $S_*^{(T)}$ is the temperature-dependent saturation mass in g.

The applied current density is the sum of the current densities of the three electrochemical reactions, are given as

$$I = i_H + i_M + i_L . \quad (3.18)$$

In conclusion, the model uses 15 variables and 15 governing equations. The variables are S_8^0, S_4^{2-}, S_2^{2-},S^{2-}, S_p, i_H, i_M, i_L, V_{cell}, η_H, η_M, η_L, E_H, E_M, E_L.

3.1. Initial Conditions

It is assumed that only the first electrochemical reaction occurs initially. The following initial conditions, that are used for the beginning of the first discharge [22] are given as

$$S_8^0 0 = m_s * 0.99, \quad (3.19)$$

$$V_{cell} = 2.5, \quad (3.20)$$

$$i_H = I, \quad (3.21)$$

$$\eta_H = \frac{2RT}{n_H F} arcsinh\left(\frac{-i_H}{2 i_H^0 a_r} \right), \quad (3.22)$$

$$E_H = V_{cell} - \eta_H, \quad (3.23)$$

$$S_4^{2-} = \left(\frac{f_H S_8^0}{exp\left(\frac{n_H F}{RT} \right) (E_H - E_H^0)} \right)^{1/2}, \quad (3.24)$$

$$i_L = 0, \quad (3.25)$$

$$\eta_L = 0, \quad (3.26)$$

$$E_L = V_{cell} - \eta_L, \quad (3.27)$$

$$i_M = 0, \tag{3.28}$$

$$\eta_M = 0, \tag{3.29}$$

$$E_M = V_{cell} - \eta_M, \tag{3.30}$$

$$S_2^{2-} = \left(\frac{f_M S_4^{2-}}{exp\left(\frac{n_M F}{RT}\right)(E_M - E_M^0)} \right)^{1/2}, \tag{3.31}$$

$$S^{2-} = \left(\frac{f_L S_2^{2-}}{exp\left(\frac{n_L F}{RT}\right)(E_L - E_L^0)} \right)^{1/2}, \tag{3.32}$$

$$S_P = m_S - S_8^0 - S_4^{2-} - S_2^{2-} - S^{2-}. \tag{3.33}$$

At the beginning of the charge, concentrations of the species and voltage at the end of the first discharge are taken as initial conditions. By definition, the value of the current density is taken as positive during discharge and negative during charge. It is assumed that only the last electrochemical reaction occurs at the beginning of the charge. The initial conditions for the first charge are shown as

$$i_H = 0, \tag{3.34}$$

$$i_M = 0, \tag{3.35}$$

$$i_L = \mathrm{I}, \tag{3.36}$$

$$\eta_H = 0, \tag{3.37}$$

$$\eta_M = 0, \tag{3.38}$$

$$\eta_L = \frac{2RT}{n_L F} arcsinh\left(\frac{-i_L}{2i_L^0 \alpha_r}\right), \tag{3.39}$$

$$E_H = V_{cell} - \eta_H, \tag{3.40}$$

$$E_L = V_{cell} - \eta_L, \tag{3.41}$$

$$E_M = V_{cell} - \eta_M. \tag{3.42}$$

3.2. Parameters Used in the Model

The parameters used in the model are mostly based on Cornish and Marinescu [22] and shown in the table below.

Table 1.1. Parameter values applied in the zero-dimensional model [1].

Name – Units	Notation	Value
Faraday's constant ($C\ mol-1$)	F	$9.649x10^4$
Molar Mass of S (g mol-1)	M_{S_8}	32
Electron number per reaction	n_H, n_M, n_L	4,2,2
Number of S atoms in polysulfide	$n_{S_8^0}, n_{S_4^{2-}}, n_{S_2^{2-}}, n_{S^{2-}}$	8,4,2,1
Gas constant (JK-1mol-1)	R	8.3145
Density of precipitated Sulfur (gL-1)	ρ_S	$2x10^3$
Active reaction area per cell (m^2)	a_r	0.960
Dimensionality factor H ($g\ L\ mol^{-1}$)	f_H	0.924
Dimensionality factor M ($g\ L\ mol^{-1}$)	f_M	0.604
Dimensionality factor L ($g\ L\ mol^{-1}$)	f_L	0.427
Electrolyte volume per cell (L)	v	0.0114
Exchange current density H ($A\ m^{-2}$)	i_H^0	5
Exchange current density M ($A\ m^{-2}$)	i_M^0	5
Exchange current density L ($A\ m^{-2}$)	i_L^0	5
Standard potential H (V)	E_H^0	2.43
Standard potential M (V)	E_M^0	2.41
Standard potential L (V)	E_L^0	1.9
Initial charge S^{2-} (g)	$S^{2-}(t=0)$	10^{-3}
Initial charge S_p (g)	$S_p(t=0)$	0.43
$30°C$ Dissolution rate (s^{-1})	$k_d^{(30)}$	5000
$30°C$ Shuttle rate (s^{-1})	$k_s^{(30)}$	10^{-4}
$30°C$ Saturation mass (s^{-1})	$S_*^{(30)}$	10^{-7}

3.3. Linearization of the Governing Equations

Fortran is utilized for establishing a computational model for the Li-S battery. First, the linearization of the equations is needed in order to run the model developed in Fortran.

The linearization process is performed for the governing equations that can be expressed as

$$a_{i,k}\ (x)\frac{dC_k^2}{dx^2} + b_{i,k}\ (x)\frac{dC_k}{dx} + d_{i,k}\ (x)\ C_k = g_i(x). \tag{3.43}$$

Here, the coefficients $a_{i,k}\ (x)$, $b_{i,k}\ (x)$, $d_{i,k}\ (x)$ and $g_i(x)$ are calculated for each equation. The subscript i indicates the equation number, and k indicates the variable number. When linearizing the equation, the applied equations can be written as

$$C_k^* = C_{kprev} + \Delta C_k, \tag{3.44}$$

$$\frac{dC_k^*}{dt^*} = \frac{\Delta C_k}{\Delta t}. \tag{3.45}$$

In order to demonstrate how the linearization process works, the first governing equation (3.13) is linearized as an example, can be expressed as

$$\frac{dS_8^0}{dt} = -\frac{M_S * n_{S_8^0}}{n_H F} i_H - k_S^{(T)} S_8^0, \tag{3.46}$$

$$S_8^0 = S_{8prev}^0 + \Delta S_8^0, \tag{3.47}$$

$$\frac{dS_8^0}{dt^*} = \frac{\Delta S_8^0}{\Delta t}, \tag{3.48}$$

$$\frac{\Delta S_8^0}{\Delta t} = -\frac{M_S * n_{S_8^0}}{n_H F} (i_{Hprev} + \Delta i_H) - k_S^{(T)} (S_{8prev}^0 + \Delta S_8^0), \tag{3.49}$$

$$\frac{\Delta S_8^0}{\Delta t} + \frac{M_S * n_{S_8^0}}{n_H F} \Delta i_H + k_S^{(T)} S_8^0 = -\frac{M_S * n_{S_8^0}}{n_H F} i_{Hprev} - k_S^{(T)} \Delta S_8^0, \tag{3.50}$$

where $b_{1,1}$ =1 , $d_{1,1} = k_S^{(T)}$, $d_{1.6} = \frac{M_S * n_{S_8^0}}{n_H F}$ and $g_1 = \frac{-M_S * n_{S_8^0}}{n_H F} i_{Hprev} - k_S^{(T)} S_{8prev}^0$.

4. RESULTS AND DISCUSSION

In this chapter, the effect of model parameters on the discharge/charge behaviour of a Li-S cell is discussed to investigate the impact of electrolyte design. The simulations of the zero-dimensional mathematical model were executed using the Fortran programming language. Sensitivity analysis was performed by changing model parameters, such as C-rate, active reaction area α_r, and shuttle constant (k_s). Additionally, simulations on the impact of the electrolyte-to-sulfur ratio were performed and analysed. Evaluations regarding the sensitivity of the model parameters were made based on cell capacity versus voltage graphs. Model parameters were changed based on the reference parameter values given in the model development section.

4.1. Sensitivity Analysis

4.1.1. The Effect of Active Reaction Area per Cell (a_r) on the Performance of Lithium-Sulfur Batteries

The active surface area of the cathode represents the surface area of the solid-liquid interface per unit volume of the porous cathode. In reality, the precipitation of lithium sulfides in the cathode reduces the electrochemically active area at the solid-liquid interface [33]. However, in the proposed model, precipitation does not affect the active surface area as it is not defined as a function of the cathode porosity [22].

The discharge profiles of Li-S batteries with different active reaction areas are graphed for a 0.1 C rate. The baseline active reaction area per cell is taken as 0.96 m^2. The impact of active surface area on cell performance was assessed by using values that were ten times and 0.1 times the reference value.

Increasing the active surface area improves sulfur utilization in the cathode by enhancing electron transfer. However, the enhancement is apparent until a specific value.

The improvement in the cell voltage is not prominent for the higher reaction area values [34] [35] [36]. The discharge voltage and capacity should increase with a higher reaction area.

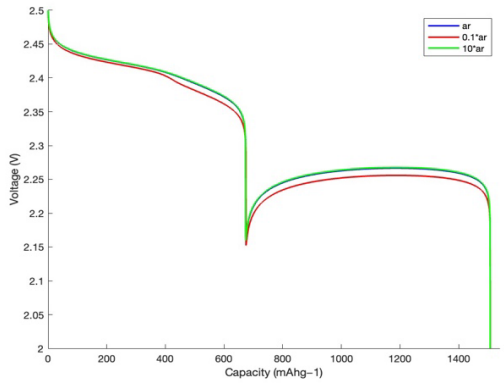

Figure 4.1. The effect of the active reaction area on voltage and cell capacity during discharge at 0.1 C rate.

According to Figure 4.1, increasing the reaction area of the cathode shows no remarkable change in cell performance and capacity during discharge. On the other hand, when the surface area of the sulfur cathode decreases, the cell voltage slightly decreases in the first and second discharge profiles. The reaction area affects the reaction rate and overpotential, as can be seen in equations 3.4 -3.9, stated in Chapter 3. On the other hand, the discharge capacity is not sensitive to a change in the active surface area in the model.

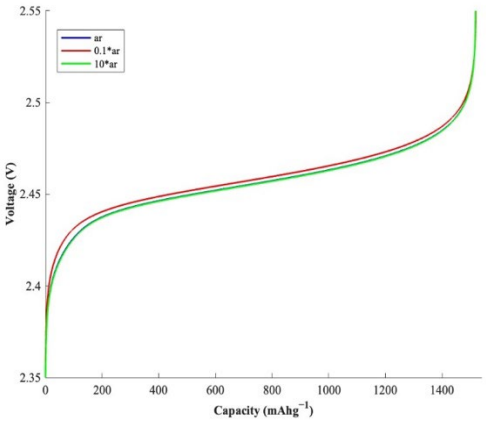

Figure 4.2. The charge voltage versus capacity simulations with various active reaction areas at 0.1 C rate.

The first charge profiles are depicted with various reaction areas in Figure 4.2. Similar to the discharge profile, an increase in the active surface area of the cathode does not make a significant change in cell capacity and voltage outputs. It is also shown that voltage outputs are higher at lower surface areas (a_r) due to increased overpotentials.

To sum up, the rate of the redox reactions that occur in the cathode strongly depends on the surface area. However, spatial variations are not considered in the zero-dimensional model. The area is assumed to be independent of the porosity. Nevertheless, porosity and area change spatially within the electrodes [37]. This may be the reason why the model results are not highly sensitive to the electrochemically active area.

4.1.2. The Effect of Initial Voltage (V_0) on the Performance of Lithium-Sulfur Batteries

Increasing the initial cell voltage enhances energy and power densities [38]. Discharge voltage increases with higher initial voltage values. However, a higher applied initial voltage value in the Li-S batteries drives electrolyte oxidation in the electrolyte-cathode interface that causes a layer between the interfaces. Hence, higher initial voltage raises the electrical resistance and lowers the electrochemical performance [39].

The first discharge profiles are depicted for various initial voltage inputs. Figure 4.3 indicates that the initial capacity of the Li-S cell increases with decreasing initial voltage value. Also, the voltage dip point decreases significantly with a lower initial voltage. On the other hand, the initial discharge profiles of $V_0 = 2.45$ and $V_0 = 2.50$ do not differ from each other.

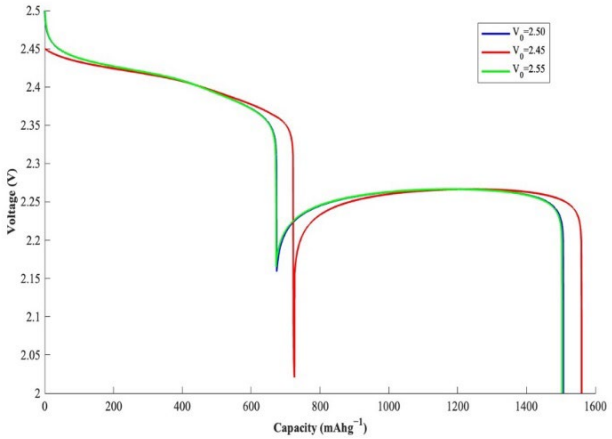

Figure 4.3. Discharge simulations for various initial cell voltage V_0 at 0.1 C-rate.

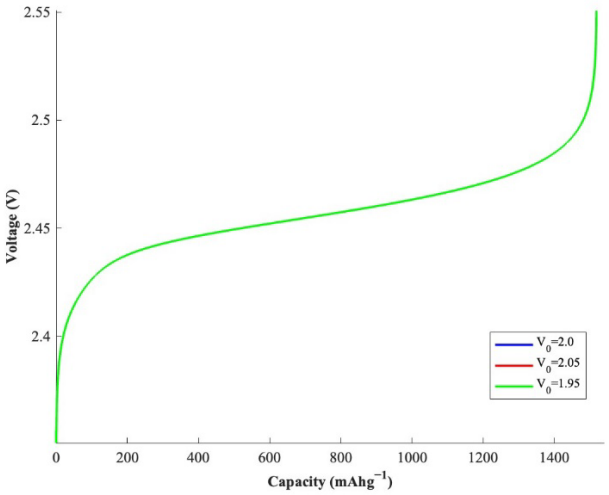

Figure 4.4. Charge simulations for various initial cell voltage V_0 at 0.1 C-rate.

The initial voltage values have no impact on the charge performance, and the voltage output values remain constant in simulations with varying initial voltage values. This may be expected since V_0 is an initial condition for the battery discharge and has no direct effect on the charge initial conditions.

4.1.3. The Effect of Shuttle Constant (k_s) on the Performance of Lithium-Sulfur Batteries

The shuttle effect of polysulfides is an undesirable phenomenon for the Li-S cell performance. Lithium polysulfide species move from the cathode to the anode to react with metallic lithium. Short-chain polysulfides are created [40]. The major drawbacks of the polysulfide shuttle phenomenon are fast capacity fade, low coulombic efficiency, and high self-discharge [41]. An increase in the shuttle constant leads to a lower discharge capacity. In the model, the shuttle effect is taken into consideration with the shuttle constant.

Discharge profiles for various shuttle constants are examined. The effect of the shuttle constant on the total discharge capacity is evident. Lower shuttle constant values display higher discharge capacities.

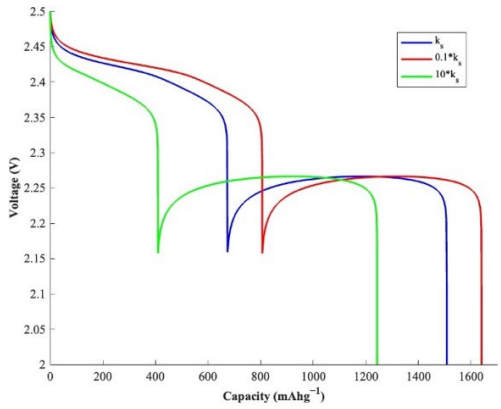

Figure 4.5. The discharge voltage versus capacity simulations with various shuttle constants with 0.1 C rate.

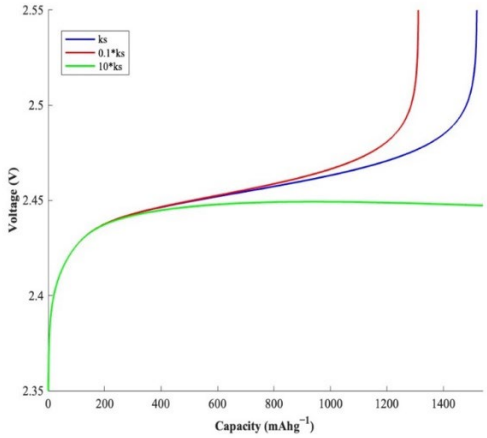

Figure 4.6. The charge voltage versus capacity simulations with various shuttle constants with 0.1 C rate.

The shuttle constant also affects the charge performance. The charge simulations with higher shuttle constants displays infinite charging. At the end of the charge profile, the effect is clearer as it leads to faster degradation and reduced Coulombic efficiency [42].

The proposed model accurately captures the impact of the polysulfide shuttle mechanism, although the shuttle effect is a space-related phenomenon. The model is successful in capturing the highly complicated shuttling mechanism with a single constant [22].

4.1.4. The Effect of Precipitation/ Dissolution Rate Constant (k_p) on the Performance of Lithium-Sulfur Batteries

The precipitation reaction reduces the concentration of S^{2-} ions in the electrolyte at a rate proportional to the precipitation constant k_p. This decrease in ionic concentration affects the electrolyte's conductivity, ultimately leading to a reduction in the cell's discharge capacity. In literature, the charge capacity depends on the system's ability to dissolve the precipitated species fast enough, as this ability impacts sulfur utilization.

The base precipitation /dissolution rate constant for discharge and charge is taken as 5000 s^{-1}. Figure 4.7 shows that simulations display high voltage plateaus for various

precipitation constants that do not differ from each other. On the other hand, the low voltage plateau shifts upward with an increase in the precipitation constant. Discharge capacities are insensitive to this model parameter.

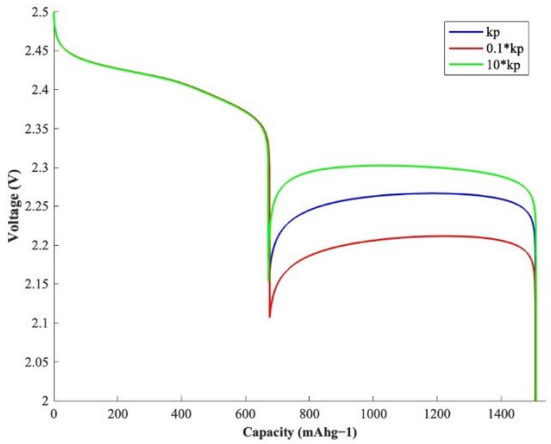

Figure 4.7. The discharge voltage versus capacity simulations with various precipitation rate constants (k_p) with 0.1 C rate.

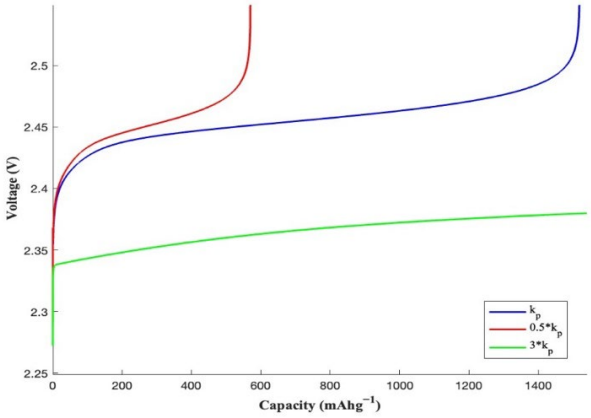

Figure 4.8. The charge voltage versus capacity simulations with various precipitation rate constants (k_p) with 0.1 C rate.

Precipitation/dissolution rate constant has an important impact on charge profiles and Li-S cell performance. Voltage outputs of charge simulations are significantly reduced with an increase in the precipitation/dissolution rate constant. The charge capacity is also affected by the constant. Charge simulations reflect that an increase in the precipitation rate constant

enhances the charge capacity. However, according to the literature, this is not expected. When precipitation increases, the charge capacity should decrease.

The discharge capacities are found to be insensitive to the precipitation constant since precipitation does not affect the active surface area and transport limitations are not considered in the proposed model.

4.1.5. The Effect of Standard Potential (E_H^0) on the Performance of Lithium-Sulfur Batteries.

In the proposed model, simulations illustrate that standard potential for high voltage plateau has a positive effect on high voltage plateau. This may be because the higher standard potential for the reduction of elemental sulfur to polysulfides speeds up the electrochemical reactions. The response of voltage outputs to standard potential increase is more evident. On the other hand, as the standard potential value rises, the change in the results of voltage output in high voltage plateau becomes less certain. The standard potential for high voltage plateau does not change the low voltage plateau significantly.

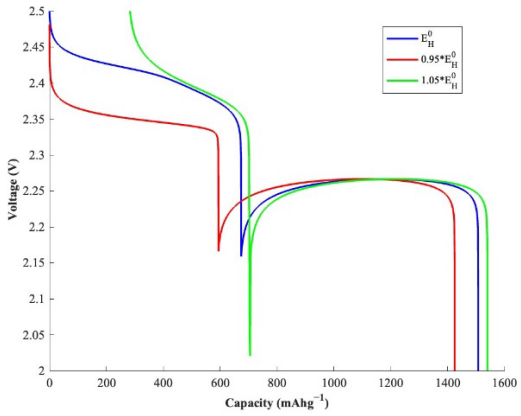

Figure 4.9. The discharge voltage versus capacity simulations with various standard potential E_H^0 with 0.1 C rate.

In the charge graphs, the effect of the standard potential on the voltage plateau is distinguishable. The voltage output during charge increases with increasing standard

potential E_H^0, as expected. The model is sensitive to changes in high voltage standard potential in initial discharge and charge.

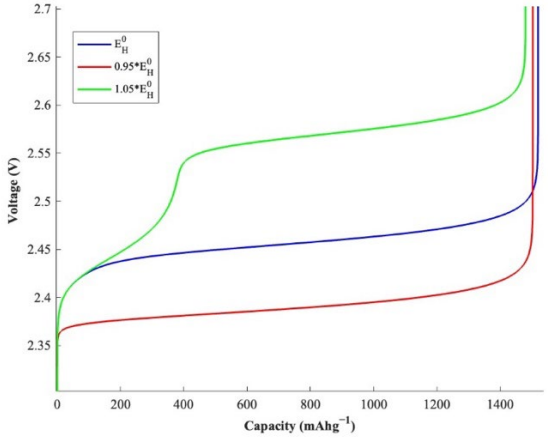

Figure 4.10. The charge voltage versus capacity simulations with various standard potential E_H^0 with 0.1 C rate.

4.1.6. The Effect of Standard Potential (E_M^0) on the Performance of Lithium-Sulfur Batteries

The influence of standard potential for the reduction of polysulfides to lower polysulfides is evaluated in Figure 4.11 and Figure 4.12. Higher values of standard potential E_M^0 do not have a significant impact at the beginning or end of the discharge process. However, the influence of the model parameter can be seen in the middle of the process. High standard potential gives lower dips in the simulations.

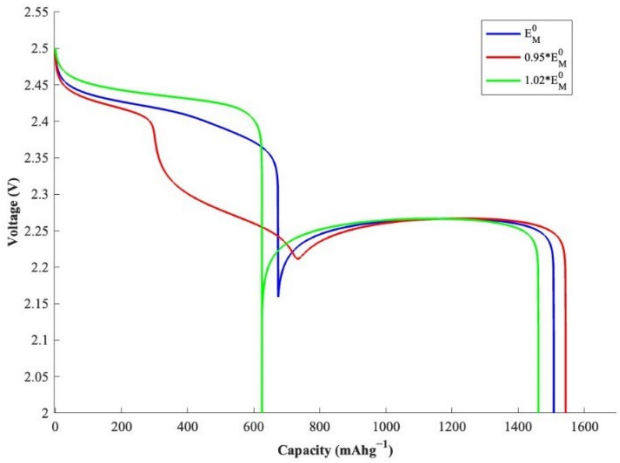

Figure 4.11. The discharge voltage versus capacity simulations with various standard potential $E_M{}^0$ with 0.1 C rate.

The effect of standard potential is less observable during the charging process. At the beginning of the charge, the voltage output increases when the standard potential increases. The charge capacity is also positively impacted by the standard potential parameter.

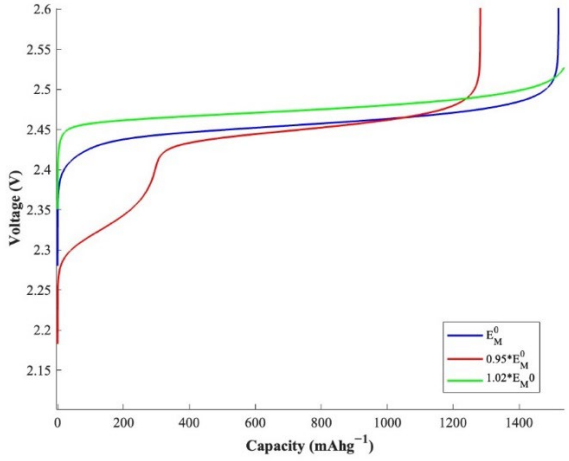

Figure 4.12. The charge voltage versus capacity simulations with various standard potential $E_M{}^0$ with 0.1 C rate.

4.1.7. The Effect of Standard Potential (E_L^0) on the Performance of Lithium-Sulfur Batteries

The standard potential of reduction of Lithium sulfide (Li_2S) to Sulfide (S^{2-}) is directly related to the lower voltage plateau. When the standard potential E_L0 increases, the reduction is more thermodynamically favorable. As a result, higher voltage profiles were observed in the low voltage plateau in the discharge graphs with higher E_L0 values. The parameter also affects the dip of the discharge profile.

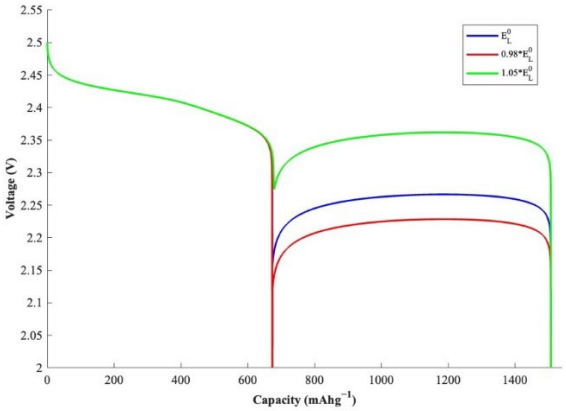

Figure 4.13. The discharge voltage versus capacity simulations with various standard potential E_L^0 with 0.1 C rate.

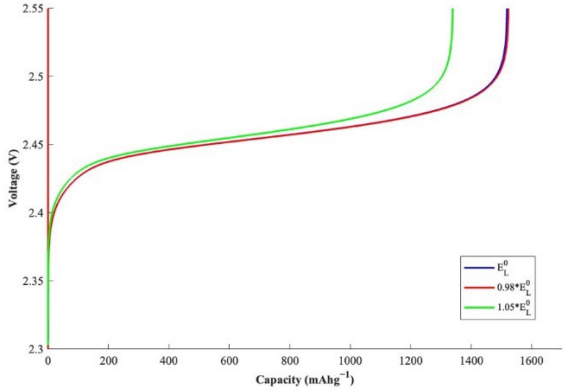

Figure 4.14. The charge voltage versus capacity simulations with various standard potential E_L^0 with 0.1 C rate.

The charge capacity decreases with an increase in the standard potential. However, in the lower standard potential values, this trend is not applicable. The results of E_L^0 and 0.98* E_L^0 are almost the same.

4.1.8. The Effect of Exchange Current Density for the High Voltage Plateau (i_H^0) on the Performance of Lithium-Sulfur Batteries

The exchange current density reflects how rapidly an electrode may participate in an electrochemical process. A larger exchange current density decreases the energy barrier that the charge requires in order to move between the electrolyte and the catalyst surface. Increasing the exchange current density improves cell performance [43].

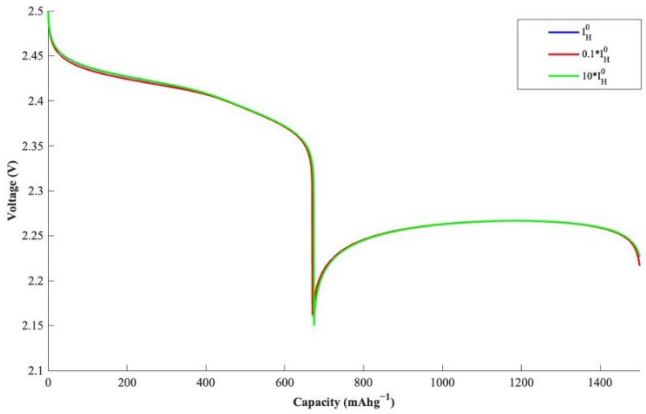

Figure 4.15. The discharge voltage versus capacity simulations with various exchange current density (i_H^0) values with 0.1 C rate.

In the proposed mathematical model, the impact of the exchange current density i_H^0 is not observed. The discharge capacity and voltage outputs remained the same while increasing the value of the model parameter i_H^0.

Similarly, the difference between charge profiles is almost unnoticeable. The charge process is also not affected by the exchange current density i_H^0, as seen in Figure 4.16.

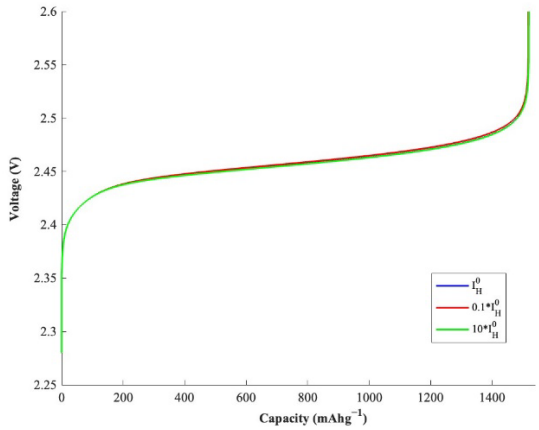

Figure 4.16. The charge voltage versus capacity simulations with various exchange current density (i_H^0) values with 0.1 C rate.

4.1.9. The Effect of Exchange Current Density (i_M0) on the Performance of Lithium-Sulfur Batteries

The discharge and charge simulations were executed for 0.1* i_M^0, i_M^0, and 10* i_M^0. As shown in Figure 4.17, it can be evaluated that the change in i_M^0 has a negligible effect on the discharge voltage output and capacity.

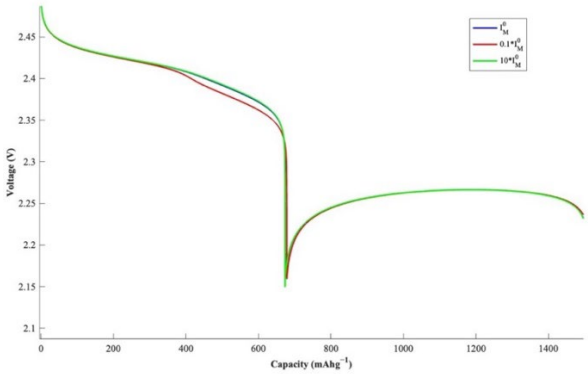

Figure 4.17. The discharge voltage versus capacity simulations with various exchange current density (i_M^0) values with 0.1 C rate.

As shown in Figure 4.18, the i_M^0 model parameter does not affect the charge versus voltage profile. The charge profiles remain almost constant regardless of changes in the

parameter for all i_M^0 values. The change in charge and discharge profiles are not captured by the model, which is unexpected.

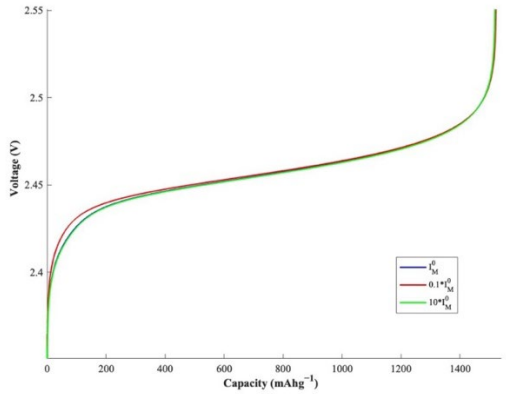

Figure 4.18. The charge voltage versus capacity simulations with various exchange current density (i_M^0) values with 0.1 C rate.

4.1.10. The Effect of Exchange Current Density for the Low Voltage Plateau (i_L^0) on the Performance of Lithium-Sulfur Batteries

The exchange current density is an important factor in the performance of lithium-sulfur batteries as it affects the kinetics of lithium polysulfide reactions. Higher exchange current densities lead to an enhancement in the rate of redox reactions. Thus, higher values improve discharge capacity and sulfur utilization [44].

Figure 4.19 illustrates the variation in the initial discharge profiles with three distinct exchange current density values. The exchange current density i_L^0 has almost no impact on capacity. Normally, the exchange current density is expected to influence the low voltage plateau. However, the model prediction is not clear enough, although the difference between i_L^0 and 0.1* i_L^0 values can be seen.

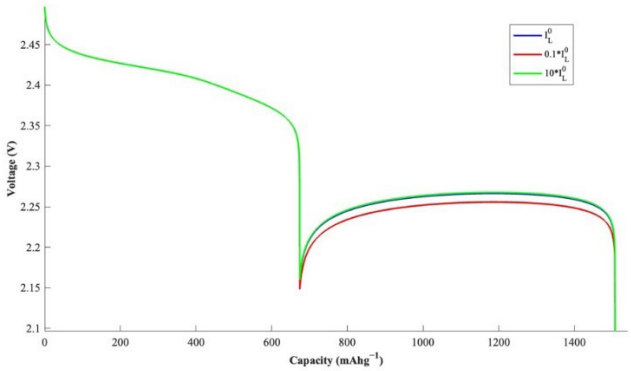

Figure 4.19. The discharge voltage versus capacity simulations with various exchange current density ($i_L{}^0$) values with 0.1 C rate.

The charge profiles also tend to show the same effect with high voltage plateau during discharge. The exchange current density $i_L{}^0$ does not have an impact on the charge voltage profile.

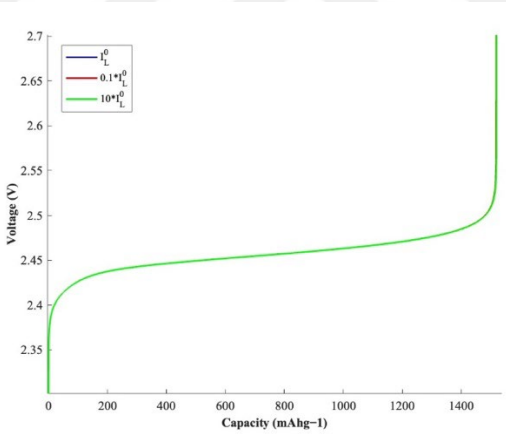

Figure 4.20. The charge voltage versus capacity simulations with various exchange current density ($i_L{}^0$) values with 0.1 C rate.

4.1.11. The Effect of C-rate on the Performance of Lithium-Sulfur Batteries

The rate at which a battery discharges over time is known as the discharge rate [45]. At lower C- rates, the time for reactions to occur in the cell is much longer than at higher C rates, which increases sulfur utilization and reduces the shuttle effect [46]. The voltage output in the low voltage plateau drops with the increase in the C rate. In addition, the dip point of the voltage curve is affected by the changes in the C rate. Discharge capacity is

slightly affected by the C-rate when 0.1C and others are compared. However, the difference between higher C rates is not significant.

A decrease in discharge capacity is expected for larger discharge rates since the limited transport properties of Li ions lead to increased polarization in the cathode, anode, and liquid electrolytes. However, the proposed model is unable to predict this trend. This may be explained by the fact that the proposed model does not consider mass transport and consequently cannot predict the capacity decrease with increasing C-rates.

The voltage drop is also expected to be enhanced at higher C-rates. This decrease in voltage output with higher C rates is expected, as in the literature [47]. At increased C-Rates, increased internal resistance becomes more noticeable, causing decreased voltage and energy efficiency [48].

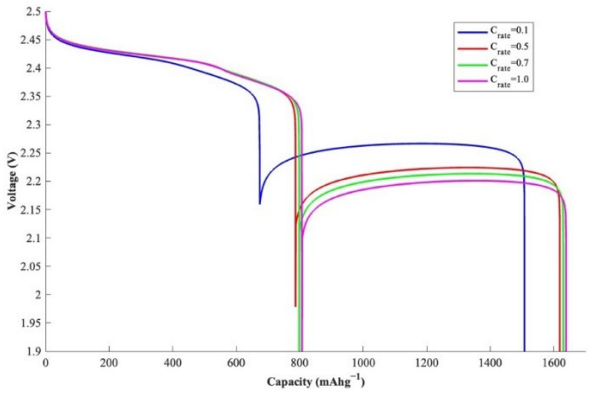

Figure 4.21. The discharge voltage versus capacity simulations with various C-rate values.

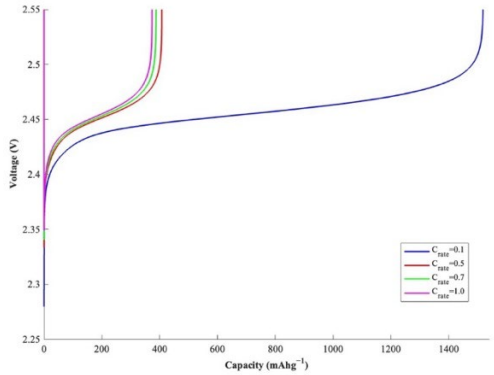

Figure 4.22. The charge voltage versus capacity simulations with various C-rate values.

The charge profiles display the expected correlation between C-rates and capacities; capacity tends to increase with decreasing C rates. To sum up, the model is unable to capture the impact of the C-rate on the discharge performance but predicts the expected trend during the charge.

4.2. Electrolyte-to-Sulfur (E/S) Ratio

The electrolyte-to-sulfur ratio can be defined as the ratio of the volume of the electrolyte to the weight of sulfur in the cathode. The effect of the E/S ratio on the predicted discharge and charge profiles is investigated by setting the sulfur loading to 2.7 g while varying the electrolyte amount between 2.7 and 81 mL. Experimental trends show that higher initial discharge capacities and increased sulfur utilization rates are achieved by increasing the E/S ratio, even though the excessive amount of electrolyte reduces energy density and enhances the polysulfide shuttle effect [49] [50].

Figure 4.23 illustrates the variations in discharge capacity for various quantities of electrolytes. The change in the E/S ratio does not clearly affect the discharge capacity in the high voltage plateau. The low voltage plateau demonstrates the influence of the parameter. An increase in the E/S ratio reduces the low plateau voltage. It was expected that the increase in the E/S ratio would change discharge capacity positively [51]. However, this trend cannot be observed during the discharge simulations.

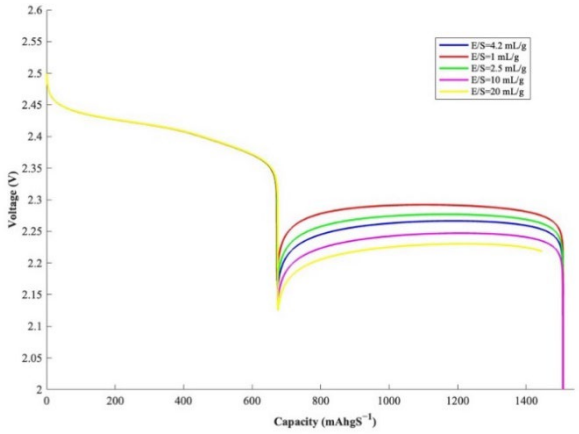

Figure 4.23. The discharge voltage versus capacity simulations with various E/S ratios at 0.1 C rate.

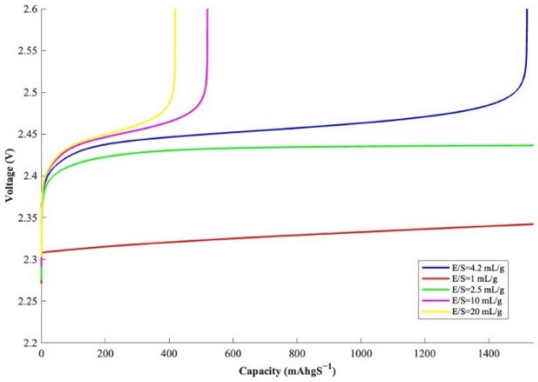

Figure 4.24. The charge voltage versus capacity simulations with various E/S ratios at 0.1 C rate.

The charge capacity increases with decreasing E/S ratio. At the lowest values of the E/S ratio, the curve transforms into a flat shape through the end of the charge, indicating infinite charging. Moreover, decreasing E/S ratios lead to lower voltage outputs during charge. It may be discussed that the 0-D model is responsive to changes in the E/S ratio during charge. On the other hand, it cannot predict the experimental trends. The model's insensitivity to the design parameter might be due to the absence of cathode porosity in the model and the sulfur dissolution reaction.

4.3. The Effect of Properties of Ionic Liquid Electrolytes on Li-S Cell Performance

Electrolyte type and design have a significant impact on the charge/discharge profile of Li-S batteries. Electrolytes can impact electrochemical reaction kinetics and battery performance. Different electrolyte types show various viscosity and polysulfide solubility properties.

The polysulfide shuttle mechanism can be minimized with high viscosity values. However, high viscous electrolytes have shortcomings, such as decreasing Li^+ transportation rate. Battery performance is more influenced by the effects of polysulfide solubility than viscosity [52]. Thus, it is so important to design electrolytes to balance these advantages and drawbacks. In the proposed model, the effect of electrolyte type and design can be seen implicitly through model parameters.

The electrolyte type and amount can affect the active surface reaction area between the electrolyte-electrode interlayer. A higher active reaction area can promote higher sulfur utilization until a threshold. Higher reaction rates increase the discharge capacity. The initial discharge voltage may also be directly related to electrolyte design. High initial voltage increases the discharge voltage but reduces charge capacity. The proposed model may capture the impact of electrolyte properties on the voltage profiles through these two model parameters, yet the change in the discharge capacity can only be predicted through a change in the initial voltage value.

The solubility of lithium polysulfides is significantly dependent on the solvent's donor ability and it impacts the reaction pathway [53]. Limiting the solvating capacity of the electrolyte solution reduces the solubility of lithium polysulfides, which in turn reduces the shuttle effect. The shuttle constant, a model design parameter, implicitly captures the shuttle effect.

An increase in the shuttle constant leads to a decrease in the discharge voltage and cell capacity. Consequently, it may be discussed that the influence of different electrolytes may be expressed through varying shuttle constants.

According to the literature, an electrolyte with a high salt content may improve the cycle stability of a Li-S cell. It also increases the concentration of dissolved Li-polysulfides in the electrolyte, which promotes irreversible precipitation and polysulfide reductions at the anode. The precipitation process lowers the concentration of S^{2-} ions in the electrolyte. This decrease in ionic concentration affects the electrolyte's conductivity, lowering the cell's discharge capacity. The precipitation constant in the model can be used to represent the influence of precipitation reactions. In the model, a higher precipitation constant lowers the low-voltage discharge plateau, which is consistent with predictions. According to the literature, charge capacity should be decreased with increasing the precipitation constant. However, in the model, the discharge capacity is unaffected by k_p since precipitation does not impact the active surface area, and transport restrictions are not included.

Concentrations of salts and solvents in the battery impact the reaction kinetics. Additionally, cation solvation energy and concentration of species play a crucial role in determining the electrode potential [54]. Equations between 3.10 and 3.12 in Chapter 3 show that Nernst potential is influenced by the concentration of species and standard potentials. Both terms are affected by the type of electrolytes. Consequently, standard potentials and Nernst potentials are related to electrolyte choice and design, and their impact on the cell performance may be captured by the sensitivity analysis through the model. An increased standard potential for high voltage plateau accelerates electrochemical processes of reduction of elemental sulfur to polysulfides. Thus, a higher standard potential (E^0_H) improves the performance of the high-voltage plateau and increases the voltage output of the first plateau during discharge. Similarly, higher standard potential values for low voltage plateaus increase the second plateau voltage during discharge. When sensitivity analysis is performed regarding standard potentials, it is seen that the model can capture the effect of the parameter on discharge and charge profiles.

An elevated concentration of polysulfides causes the electrolyte to become more viscous, which can influence reaction rates and ionic transport by decreasing ion mobility. The model's exchange current densities may be able to implicitly depict this event. The exchange current density positively impacts the active material utilization and lowers overpotential, which results in an increase in the discharge capacity. The model is not

sensitive to the exchange of current densities since the impact on the charge and discharge profiles is not expected as in the literature. The change in the exchange current density values does not alter the discharge and charge profiles.

The electrolyte-to-sulfur ratio is directly related to the electrolyte amount and electrolyte properties. Increasing the electrolyte amount increases sulfur utilization. Thus, discharge capacity increases until a threshold is reached since excessive amounts of electrolytes enhance the polysulfide shuttle effect and reduce energy density. In the model, the charge capacity increases with decreasing E/S ratio. At the lowest values of the E/S ratio, the curve transforms into a flat shape through the end of the charge, indicating infinite charging. It can be concluded that the effect of the E/S ratio on the cell performance cannot be expressed with the proposed model.

5. CONCLUSIONS

A zero-dimensional electrochemical model is used in this study to examine the impact of electrolyte design on the Li-S cell performance. The evaluations were performed via sensitivity analysis, and the E/S ratio was changed at a constant temperature. Except for the simulations on the impact of C-rates, the simulations were performed with a constant C-rate of 0.1C. The sulfur loading also did not change during the study. The simulations were made to predict voltage versus capacity profiles of discharge and charge processes. Due to the zero dimensionality, the model is not space dependent. However, the shuttle effect is taken into consideration. The reduction of elemental sulfur to sulfide is considered through a three-stage electrochemical reaction mechanism in the model.

The model does not predict varying discharge and charge profiles with changing active reaction area and initial voltage value. The changes in the voltage versus capacity curves for various reaction areas and initial voltage values are negligible. On the other hand, the model projects that the shuttle constant has a significant effect on capacity and voltage.

The effect of standard potentials for three redox reactions was also investigated. The model is relatively accomplished in predicting the impact of the standard potentials on discharge and charge performance. Increasing the standard potentials leads to higher voltage outputs and capacity for all reactions.

A sensitivity analysis for the exchange of current densities for all three electrochemical reactions mentioned in the model is conducted. The model is unsuccessful in predicting the impact of exchange current densities on cell performance for all three reactions. Since higher exchange current densities improve reaction kinetics, both voltage and capacity should be increased; yet the model results do not project this trend.

Accurate predictions of the Li S cell's discharge performance as a function of C-rate cannot be made with the proposed model. This is mainly due to neglecting mass transfer in a zero-dimensional model.

The proposed model failed to predict the discharge behaviour of Li-S cells when evaluating the impact of the electrolyte-to-sulfur ratio. Discharge capacity is known to increase with increasing E/S ratios until a certain threshold. Discharge simulations do not reflect the effect of the E/S ratio on discharge capacity, although voltage increases with the E/S ratio in the demonstrated simulations.

In conclusion, the model is mostly successful in capturing the changes in the plateau voltages for various model parameters. On the other hand, predicted discharge capacities are only sensitive to the shuttle constant in the model, which makes it hard to model the effect of electrolyte type and properties on the discharge capacity. The model dimension can be considered as one of the reasons behind this. Since the mass transport that occurred in the electrolyte were not taken into consideration in the zero-dimensional model, erroneous predictions may have been made in the simulations, especially regarding the effect of C-rate.

For future research, higher dimensional electrochemical models could be suggested to clarify the influence of the various electrolyte design parameters discussed in this study. Because of the simplifications in this model, certain model parameters have not been accurately analysed. The model proposed that electrochemical reactions occurred during discharge may classified as three-step reactions. Thus, multi-step reactions of more than three can be evaluated for improving the model sensitivity. Additionally, sulfur dissolution can be considered to capture more accurate charge and discharge profiles for investigating the impact of the electrolyte-to-sulfur ratio.

REFERENCES

1. Goodenough J. B., and Y. Kim, "Challenges for Rechargeable Li Batteries", *Chemistry Of Materials,* Vol. 22, No. 3, pp. 587-603, 2010.

2. Li, G., Z. Chen ,and J. Lu, "Lithium-Sulfur Batteries for Commercial Applications", *Chem,* Vol. 4, No. 1, pp. 3-7, 2018.

3. Etacheri, V., R. Marom, R. Elazari, G. Salitra, and D. Aurbach, "Challenges in the Development of Advanced Li-Ion Batteries: A Review", Energy & Environmental Science, Vol. 4, No. 9, pp. 3243-3262, 2011.

4. Kubota, K., M. Dahbi, T. Hosaka, S. Kumakura, and S. Komaba, "Towards K-Ion and Na-Ion Batteries as “Beyond Li-Ion”, *The Chemical Record,* Vol. 18, No. 4, pp. 459-479.

5. Aurbach, D., Y. Talyosef, B. Markovsky, E. Markevich, E. Zinigrad, L. Asraf, J. S. Gnanaraj, and H.-J. Kim, "Design of Electrolyte Solutions for Li and Li-Ion Batteries: A Review", *Electrochimica Acta,* Vol. 50, No. 2–3, pp. 247-254, 2004.

6. Angulakshmi , N., and A. M. Stephan, " Efficient Electrolytes for Lithium–Sulfur Batteries", *Frontiers In Energy Research,* Vol. 3, p.17, 2015.

7. Bruce, P. G., S. A. Freunberger, L. J. Hardwick, and J.-M. Tarascon, "Li-O2 and Li-S Batteries with High Energy Storage", *Nature Materials,* Vol. 11, No.1, pp. 19-29, 2011.

8. Barghamadi, M., A. Kapoor, and C. Wen, "A Review On Li-S Batteries as A High Efficiency Rechargeable Lithium Battery", *Journal Of The Electrochemical Society,* Vol. 160, No. 8, p. A1256*,* 2013.

9. Kilic, A., Ç. Odabaşı, R. Yildirim, and D. Eroglu, "Assessment of Critical Materials and Cell Design Factors for High Performance Lithium-Sulfur Batteries Using Machine Learning", *Chemical Engineering Journal,* Vol. 390, p. 124117, 2020.

10. Manthiram, A., Y. Fu, and Y.-S. Su, "Challenges and Prospects of Lithium Sulfur Batteries", *Accounts Of Chemical Research,* Vol. 46, No. 5, p. 1125–1134, 2012.

11. Manthiram, A., Y. Fu, S.-H. Chung, C. Zu, and Y.-S. Su, "Rechargeable Lithium-Sulfur Batteries", *Chemical Reviews,* Vol. 114, No. 23, pp. 11751-11787, 2014.

12. Rana, M., S. A. Ahad, M. L. A, B. Luo, L. Wang, I. Gentle, and R. Knibbe, "Review on Areal Capacities And Long-Term Cycling Performances of Lithium Sulfur Battery at High Sulfur Loading", *Energy Storage Materials,* Vol. 18, pp. 289-310, 2019.

13. Lim, G. S., W. Kim, D. C. Jo, and P. J. Lee, "A Comprehensive Review of Materials With Catalytic Effects In Li-S Batteries: Enhanced Redox Kinetics", *Angewandte Chemie International Edition,* Vol. 58, No. 52, pp. 18746-18757, 2019.

14. Yang, X., X. Li, K. Adair, H. Zhang, and X. Sun, "Structural Design of Lithium–Sulfur Batteries: From Fundamental Research To Practical Application", *Electrochemical Energy Reviews ,* Vol. 1, No. 3, pp. 239–293, 2018.

15. Hofmann, A. F., D. N. Fronczek, and W. G. Bessle, "Mechanistic Modeling of Polysulfide Shuttle and Capacity Loss In Lithiumesulfur Batteries", *Journal of Power Sources,* Vol. 259, pp. 300–310, 2014.

16. Huang, Y., L. Lin, C. Zhang, L. Liu, Y. Li, Z. Qiao, J. Lin, Q. Wei, L. Wang, Q. Xie ,and D.-L. Peng, "Recent Advances and Strategies Toward Polysulfides Shuttle Inhibition for High-Performance Li-S Batteries", *Advanced Science,* Vol. 9, No. 12, p. 2106004, 2022.

17. Liu, T., Y. Elias, J. Meng, D. Aurbach, R. Zou, D. Xia, and Q. Pang, "Electrolyte Solutions Design for Lithium-Sulfur Batteries", *Joule,* Vol. 5, No. 9, pp. 2323-2364, 2021.

18. Talian, S. D., M. B. Rogac, and R. Dominko, " The Physicochemical Properties of A [Deme][Tfsi] Ionic Liquid-Based Electrolyte and Its Influence On The Performance of Lithium–Sulfur Batteries", *Electrochimica Acta,* Vol. 252, No. 16, pp. 147-153, 2017.

19. Suo, L., Y.-S. Hu, H. Li, M. Armand, and L. Chen, "A New Class Of Solvent-In-Salt Electrolyte for High-Energy Rechargeable Metallic Lithium Batteries", *Nature Communications,* Vol. 4, No. 1, p. 1481, 2013.

20. Lu, H., Y. Zhu, B. Zheng, H. Du, X. Zheng, C. Liu, Y. Yuan, J. Fang, and K. Zhang, "A Hybrid Ionic Liquid-Based Electrolyte for High-Performance Lithium–Sulfur Batteries", *New Journal Of Chemistry,* Vol. 44, No. 2, pp. 361-368, 2020.

21. Zhang, S., K. Ueono, K. Dokko, and M. Watanabe, " Recent Advances In Electrolytes for Lithium–Sulfur Batteries", *Advanced Energy Materials,* Vol. 5, No. 16, p. 1500117, 2015.

22. Cornishz M., and M. Marinescu, "Toward Rigorous Validation Of Li-S Battery Models", *Journal of The Electrochemical Society,* Vol. 169, No. 6, p. 060531, 2022.

23. Park, J. W., K. Ueno, N. Tachikawa ,and K. W. Dokko, "Ionic Liquid Electrolytes for Lithium–Sulfur Batteries", *The Journal of Physical Chemistry C,* Vol, 117, No. 40, pp. 20531–20541, 2013.

24. Zhang, S. S., "Liquid Electrolyte Lithium/Sulfur Battery: Fundamental Chemistry, Problems and Solutions", *Journal of Power Sources,* Vol. 231, p. 153–162, 2013.

25. Zhang, S. S., "Improved Cyclability of Liquid Electrolyte Lithium/Sulfur Batteries By Optimizing Electrolyte/Sulfur Ratio", *Energies,* Vol. 5, No. 12, pp. 5190-5197, 2012.

26. Chen, J., K. S. Han, W. A. Henderson, K. C. Lau, M. Vijayakumar, T. Dzwiniel, H. Pan, L. A. Curtiss, J. Xiao, K. T. Mueller, Y. Shao, and J. Li, "Restricting The Solubility of Polysulfides In Li-S Batteries via Electrolyte Salt Selection", *Advanced Energy Materials,* Vol. 6, No. 11, p. 1600160, 2016.

27. Shin J. H., and E. J. Cairns, "Characterization of N-Methyl-N-Butylpyrrolidinium Bis(Trifluoromethanesulfonyl)Imide-Litfsi-Tetra(Ethylene Glycol) Dimethyl Ether Mixtures As A Li Metal Cell Electrolyte," *Journal of The Electrochemical Society ,* Vol. 155, No. 5, pp. A368-A373, 2008.

28. Lu, H., Z. Chen, Y. Yuan, H. Du, J. Wang, X. Liu, Z. Hou, K. Zhang, J. Fang, and Y. Qu, "A Rational Balance Design of Hybrid Electrolyte Based on Ionic Liquid and Fluorinated Ether in Lithium Sulfur Batteries", *The Electrochemical Society ,* Vol. 166, No. 12, pp. A2453- A2458, 2019.

29 Peng, Y., R. Badam, T. P. Jayakumar, W. Wannapakdee, C. Changtong, and N. Matsumi, "Drastic Effect Of Salt Concentration in Ionic Liquid on Performance of Lithium Sulfur Battery", *Journal of The Electrochemical Society,* Vol. 169, No. 5, p. 050515, 2022.

30. Selvi, M. P., R. N. Elizabeth, S. Sinthika, S. A. S. Paniyarasi, S. Padmaja, and S. S. V. Backiyaleela, "Lithium-Sulfur Batteries with Triethylsulfoniumbis(Trifluoromethane Sulfonyl)Imide Ionic Liquid Duringfirst Charge-Discharge Cycling: Eis & Dft Study", *Batteries & Supercaps,* Vol. 7, No. 2, p. e202300433, 2023.

31. Marinescu, M., T. Zhang, and G. J. Offer, "A Zero Dimensional Model of Lithium–Sulfur Batteries During Charge and Discharge", *Physical Chemistry Chemical Physics,* Vol. 18, No. 1, pp. 584-593, 2016.

32. Reimer, U., Y. Holade, W. Lehnert, and B. Kokoh, "Chapter 2 - Irreversible Losses in Fuel Cells", *Fuel Cells and Hydrogen*, Second Edition, Elsevier, pp. 15-40, Amsterdam, Oxford and Cambridge, 2018

33. Kumaresan, K., Y. Mikhaylik, and R. E. White, "A Mathematical Model for A Lithium–Sulfur Cell", *Journal of The Electrochemical Society,* Vol. 155, No. 8, pp. A576-A582, 2008.

34. Eroğlu D., and N. Erisen, "Modeling The Discharge Behavior of A Lithium-Sulfur Battery", *International Journal of Energy Research,* Vol. 44, No. 13, pp. 10599–10611, 2020.

35. Eroğlu, D., S. C. Erensoy, N. B. Emerce, and N. Erisen, "Modeling The Effect of Key Cathode Design Parameters on The Electrochemical Performance of A Lithium-Sulfur Battery", *International Journal of Energy Research,*Vol, 42, No. 8, pp. 2631-2642, 2018.

36. Eroğlu, D., K. R. Zavadil, and K. G. Gallagher, "Critical Link Between Materials Chemistry and Cell-Level Design for High Energy Density and Low Cost Lithium-Sulfur Transportation Battery", *Journal of The Electrochemical Society,,* Vol. 162, No. 6, pp. A982-A990, 2015.

37. König, S., M. Suriyah, and T. Leibfried, "Validating and Improving A Zero-Dimensional Stack Voltage Model of The Vanadium Redox Flow Battery", *Journal of Power Sources,* Vol. 378, pp. 10-18, 2018.

38. Wongittharom, N., T. C. Lee, I. M. Hung, S. W. Lee, Y. C. Wang, and J. K. Chang, "Ionic Liquid Electrolytes for High-Voltage Rechargeable Li/LiNi 0.5Mn 1.5 O 4 Cells", *Journal of Materials Chemistry A,* Vol. 2, No. 10, pp. 3613–3620 , 2014.

39. Park, J. Y., M. Jo, S. Hong, S. Park, J.H. Park, Y. I. Kim, S. O. Kim, K. Y. Chung, D. Byun, S. M. Kim, and W. Chan, "Mechanism of Degradation of Capacity and Charge/Discharge Voltages of High-Ni Cathode During Fastlong-Term Cycling Without Voltage Margin", *Advanced Energy Materials,* Vol. 12, No. 29, p. 2201151, 2022.

40. Donato, G. D., T. Ates, H. Adenusi, A. Varzi, M. A. Navarra, and S. Passerini, "Electrolyte Measures to Prevent Polysulfide Shuttle Inlithium-Sulfur Batteries", *Batteries & Supercaps,* Vol. 5, No. 7, p. e202200097, 2022.

41. Knap, V., D.I. Stroe, M. Swierczynski, R. Purkayastha, K. Propp, R. Teodorescu, and E. Schaltz, "A Self-Discharge Model of Lithium-Sulfur Batteries Based on Direct Shuttle Current Measurement", *Journal of Power Sources,* Vol. 336, pp. 325-331, 2016.

42. Hua, X., T. Zhang, G. J. Offer, and M. Marinescu,"Towards Online Tracking of The Shuttle Effect in Lithium Sulfur Batteries Using Differential Thermal Voltammetry", *Journal of Energy Storage,* Vol. 21, pp. 765-772, 2019.

43. Barbir, F., "Fuel Cell Electrochemistry", *Pem Fuel Cells Theory and Practice*, Second Edition, Elsevier Academic Press, pp. 33-72, Burlington, 2012.

44. Kong, L., J. X. Chen, H. J. Peng, J. Q. Huang, W. Zhu, Q. Jin, B. Q. Li, X. Zhang, and Q. Zhang, "Current-Density Dependence 0f Li^2s/Li^2s^2 Growth in Lithium–Sulfur Batteries", *Energy & Environmental Science,* Vol. 12, No. 10, pp. 2976-2982, 2019.

45. Xingxing , W., C. Yuhang, C. Linfei, L. Shengren, Z. Yu, and D. Yelin , "The Impact of Wide Discharge C-Rates on the Voltage Plateau Performance of Cylindrical Ternary Lithium-Ion Batteries", *Energies,* Vol. 17, No. 14, p. 3488, 2024.

46. Palissat, G., "Lithium-Sulphur Batteries: Opportunities and Challenges for Space Applications", *8 The European Conference for Aeronautics and Space Sciences (Eucass),* Spain, pp. 1-12, 2019.

47. Fronczek, D. N., and W. G. Bessler, "Insight into Lithiumesulfur Batteries: Elementary Kinetic Modeling and Impedance Simulation", *Journal of Power Sources,* Vol. 244, pp. 183-188, 2013.

48. Yüksek G., and A. Alkaya, "Effect of The Depth of Discharge and C-Rate On Battery Degradation and Cycle Life", In *2023 14th International Conference On Electrical and Electronics Engineering (Eleco)*, Bursa, pp. 1-5, 2023.

49. Eroğlu D., and H. M. Bilal, "Assessment of Li-S Battery Performance as A Function of Electrolyte-To-Sulfur Ratio," *Journal of The Electrochemical Society,* Vol. 168, No. 3, p. 30502, 2021.

50. Hagen, M., P. Fanz, and J. Tübke, "Cell Energy Density and Electrolyte/Sulfur Ratio In Li–S Cells", *Journal of Power Sources,* Vol. 264, pp. 30-34, 2014.

51. Brückner, J., S. Thieme, H. T. Grossmann, S. Dörfler, H. Althues, and S. Kaskel, "Lithium-Sulfur Batteries: Influence Of C-Rate, Amount of Electrolyte and Sulfur Loading on Cycle Performance", *Journal of Power Sources,* Vol. 268, pp. 82–87, 2014.

52. Kilic, A., O. Abdelaty, M. Zeeshan, A. Uzun, R. Yildirim, and D. Eroglu, "Selection of Ionic Liquid Electrolytes for High-Performing Lithium-Sulfur Batteries: An Experiment-Guided High-Throughput Machine Learning Analysis", *Chemical Engineering Journal,* Vol. 490, p. 151562, 2024.

53. Gu, S., C. Sun, D. Xu, Y. Lu, J. Jin, and Z. Wen, "Recent Progress in Liquid Electrolyte-Based Li–S Batteries: Shuttle Problem and Solutions", *Electrochemical Energy Reviews,* Vol. 1, No. 4, pp. 599-624, 2018.

54. Cengiz, E. C., J. Rizell, M. Sadd, A. Matic, and N. Mozhzhukhina, "Review—Reference Electrodes in Li-Ion and Next Generation Batteries: Correct Potential Assessment, Applications and Practices", *Journal of The Electrochemical Society,* Vol. 168, No. 12, p. 120539, 2021.

APPENDIX A: FORTRAN CODE FOR DISCHARGE PROCESS

```
implicit none
DOUBLE PRECISION A , B , CPRev  , D , D2Cdx2 , DCDx , SMA, SMB, SMD, SMG,
SME, SMP,SMF, &
& delc , delt , G , h , time ,c1 , c2 , c3 , c4 , c5 , c6 , c7 ,c8 ,c9, c10 , c11, c12,c13, c14,c15
,&
& TON , X , XX , Y, S8in, S4in , S2in, S_in, ms , current,c_rate ,&
& R, F, T, kp, ar, fh, fm,fl, iM0, EM0, nh, nm, nl, ns8, ns4 , ns2, ns, XMAx
INTEGER it ,i, j , N , NJ , Numbertimesteps

COMMON A(15,15) , B(15,15) , DELc(15,903) , D(15,31) , G(15) , X(15,15) , Y(15,15)

COMMON/small/  SMA(16,16) , SMB(16,16) , SMD(16,16) , SMG(16) , &
& SME(16,16) , SMP(16,16) , SMF(16)

COMMON /var / CPRev(15,903) , DCDx(15) , D2Cdx2(15) , kp
COMMON /misc/ xx(1001), delt, time
COMMON /pars/ ton, xmax
COMMON /ints/ n, nj, Numbertimesteps


OPEN (70,FILE='ref-Discharge-0.1C-1.txt',STATUS='unknown')
OPEN (73,FILE='ref-Discharge-0.1C-2.txt',STATUS='unknown')
OPEN (71, FILE='ref-Discharge-0.1C_capacityandvoltage.txt',STATUS='unknown')
   time=0.0
   delt= 0.1
   CALL READ_DATA(h)
   CALL INTIAL_CONDITION(h)
   DO it = 1 , NUMbertimesteps
   CALL BOUND_VAL(h)
   time = time + delt
   DO j = 1 , NJ
```

```
c1=Cprev(1,j)
c2=Cprev(2,j)
c3=Cprev(3,j)
c4=Cprev(4,j)
c5=Cprev(5,j)
c6=Cprev(6,j)
c7=Cprev(7,j)
c8=Cprev(8,j)
c9=Cprev(9,j)
c10=Cprev(10,j)
c11=Cprev(11,j)
c12=Cprev(12,j)
c13=Cprev(13,j)
c14=Cprev(14,j)
c15=Cprev(15,j)

   if (c1.lt.0.0) then
   c1=1.0E-50
   Cprev(1,j)=c1
 end if

   if (c2.lt.0.0) then
      c2=1.0E-50
   cprev(2,j)=c2
 end if

   if (c3.lt.0.0) then
   c3=1.0E-50
   cprev(3,j)=c3
 end if

   if (c4.lt.0.0) then
      c4=1.0E-50
```

```
      cprev(4,j)=c4
 end if

   if (c5.lt.0.0) then
   c5=1.0E-50
   cprev(5,j)=c5
end if



   if (c6.le.0.0) then
      c6=0.0
      cprev(6,j)=c6
end if
   if (c7.le.0.0) then
      c7=0.0
      cprev(7,j)=c7
end if
   if (c8.le.0.0) then
      c8=0.0
      cprev(8,j)=c8
end if

   if (c9.lt.0.0) then
      c9=1.0E-50
      cprev(9,j)=c9
end if

   if (c13.lt.0.0) then
      c13=1.0E-50
      cprev(13,j)=c13
end if
```

```
    if (c14.lt.0.0) then
       c14=1.0E-50
       cprev(14,j)=c14
end if

    if (c15.lt.0.0) then
       c15=1.0E-50
       cprev(15,j)=c15
end if

    if (c10.ge.-1.0E-20) then
     c10=-0.1E-50
     cprev(10,j)=c10
end if

    if (c11.ge.0.0) then
     c11=-1.0E-20
     cprev(11,j)=c11
end if

   if (c12.ge.0.0) then
     c12=-1.0E-20
     cprev(12,j)=c12
end if



    if (c1.gt.2.7) then
    c1=2.7
    cprev(1,j)=c1
end if

    if (c2.gt.2.7) then
```

```
   c2=2.7
   cprev(2,j)=c2
end if

   if (c3.gt.2.7) then
   c3=2.7
   cprev(3,j)=c3
end if
   if (c4.gt.2.7) then
   c4=2.7
   cprev(4,j)=c4
end if
   if (c5.gt.2.7) then
   c5=2.7
   cprev(5,j)=c5
 end if

END DO


   DO j = 1 , nj
   if (j.eq.nj) then

write(70,910)time,xx(j),cprev(1,j),cprev(2,j),cprev(3,j),&
&cprev(4,j),cprev(5,j),cprev(6,j),cprev(7,j), cprev(8,j),&
&cprev(9,j)
910 FORMAT (11(G12.6,1X))
write(73,913)time,xx(j),cprev(10,j), cprev(11,j),cprev(12,j),cprev(13,j),&
&cprev(14,j),cprev(15,j)
913 FORMAT (8(G12.6,1X))
WRITE (71,911) (1675.0/(3600.0/0.1))*(time), cprev(9,j)
911 FORMAT (2(G12.6,1X))
 end if
```

```
      END DO
      END DO
      END
      !************************************************
      ! USER SPECIFIES


      SUBROUTINE READ_DATA(H)
      IMPLICIT NONE
      !*--READ_DATA54
      !*** Start of declarations inserted by SPAG
      DOUBLE PRECISION A , B , CPRev , D , D2Cdx2 , DCDx , Delc , Delt , G , H  , TON
     , X , &
      & XMAx , XX , Y , ms, R , F , T, kp,time,&
      & SMA, SMB, SMD, SMG, SME, SMP, SMF,  fh, fm,fl, iM0, EM0
      INTEGER j , N , NJ , Numbertimesteps
      !*** End of declarations inserted by SPAG
      COMMON A(15,15) , B(15,15) , DELc(15,903) , D(15,31) , G(15) , X(15,15) , &
      & Y(15,15)
      COMMON /SMALL / SMA(16,16) , SMB(16,16) , SMD(16,16) , SMG(16) , &
      & SME(16,16) , SMP(16,16) , SMF(16)
      COMMON /var / CPRev(15,903) , DCDx(15) , D2Cdx2(15), kp
      COMMON /MISC / DELt , XX(1001), time
      COMMON /PARS / TON , XMAx
      common/ints/ n, nj, Numbertimesteps



      N=15
      NJ=401
      Numbertimesteps= 36000*10
      TON= 36000
```

```
XMAx=1.0

!_____________________________________
! N is the number of unknown
! NJ is the number of node points
! xmax is the length of the domain
! Ton is the duration of the simulation
!_____________________________________________


DELt = TON/FLOAT(Numbertimesteps)
H = XMAx/FLOAT(NJ-1)
DO j = 1 , NJ
XX(j) = H*FLOAT(j-1)
if(j.eq.NJ) then
   XX(j)=xmax
end if
ENDDO
END


SUBROUTINE INTIAL_CONDITION(H)
IMPLICIT NONE

!*** Start of declarations inserted by SPAG
DOUBLE PRECISION A , B , CPRev , D , D2Cdx2 , DCDx , Delc , G ,kp,xx,delt,
time,ton,xmax, &
& H , X , Y , S8in, S4in , S2in, S_in, Spin, IHin, ILin, Vin , current, c_rate, &
& F, R, T, ms, SMA, SMB, SMD, SMG, SME, SMP, SMF, ar, fh, fm,fl, iH0, iL0,iM0,
EM0, EL0, EH0
INTEGER j , N , NJ, i,Numbertimesteps
```

```
!*** End of declarations inserted by SPAG
COMMON A(15,15) , B(15,15) , DELc(15,903) , D(15,31) , G(15) , X(15,15) , &
& Y(15,15)
COMMON /SMALL / SMA(16,16) , SMB(16,16) , SMD(16,16) , SMG(16) , &
& SME(16,16) , SMP(16,16) , SMF(16)

COMMON /var / CPRev(15,903) , DCDx(15) , D2Cdx2(15), kp
common/misc/ xx(1001), delt, time
common/pars/ ton, xmax
common/ints/ n, nj, Numbertimesteps

ms=2.7
F = 96490! f
R = 8.3145 !JK-1mol-1
T = 303.15 !Kelvin
ar=0.96 !m2
c_rate=0.1
current =ms*1.675*c_rate
fH=0.924   !gLmol-1
fM=0.604   !gLmol-1
fL=0.427   !gLmol-1
EH0=2.43      !Volt
EM0= 2.41     !Volt
EL0=1.9       !Volt
iH0=5.0       !Am-2
iM0=5.0       !Am-2
iL0=5.0       !Am-2


!INITIAL CONDITIONS

DO j = 1 , nj
CPRev(1,j) = ms*0.99
```

```
CPRev(6,j) = current
CPRev(7,j) = 0.0
CPRev(8,j) = current-CPRev(6,j)-CPRev(7,j)
CPRev(9,j) = 2.50
CPRev(10,j) = (asinh(-CPRev(6,j)/(2.0*iH0*ar)))*(2.0*R*T/(4.0*F))
CPRev(11,j) = 0.0
CPRev(12,j) = 0.0
CPRev(13,j) = CPRev(9,j) - CPRev (10,j)
CPRev(14,j) = CPRev(9,j)
CPRev(15,j) = CPRev(9,j)
CPRev(2,j) = SQRT(fh*CPRev(1,j)/exp(((CPRev(13,j)-EH0)/(R*T))*4.0*F))
CPRev(3,j) = SQRT(fm*CPRev(2,j)/exp(((CPRev(14,j)-EM0)/(R*T))*2.0*F))
CPRev(4,j) = SQRT(fl*CPRev(3,j)/exp(((CPRev(15,j)-EL0)/(R*T))*2.0*F))
CPRev(5,j) = ms-CPRev(1,j)-CPRev(2,j)-CPRev(3,j)-CPRev(4,j)



IF ( j.EQ.1 ) THEN
do i= 1 , 15
print*, CPRev(i,j)
ENDDO
ENDIF
ENDDO
END



SUBROUTINE FILLMAT(H,J)
IMPLICIT NONE
!*--FILLMAT117

DOUBLE PRECISION A , B , CPRev  , D , D2Cdx2 , DCDx , &
```

```
    & DELc , delt , G , H , SMA , SMB , SMD , SME , SMF , SMG , SMP , ks , MS8 , &
    & c1,c2,c3,c4,c5,c6, c7, c8, c9, c10, c11, c12, c13, c14, c15, &
    & NA , ne , ns8 , ns4 , ns2 , ns , R , rhos , &
    & fh , fl , v , ms , EH0 , EL0 , iH0 , iL0 , Satmass, &
    & kp , S8in, S4in , S2in, S_in, Spin, IHin, ILin, Vin, &
    & current, c_rate,  F, T , time, ar,  fm, iM0, EM0, nh, nm,nl , nu

    DOUBLE PRECISION TON , X , XMAx , XX , Y
    INTEGER ic , J , N , NJ , Numbertimesteps , i


    COMMON A(15,15) , B(15,15) , DELc(15,903) , D(15,31) , G(15) , X(15,15) ,
Y(15,15)
    COMMON /var / CPRev(15,903) , DCDx(15) , D2Cdx2(15), kp
    COMMON /SMALL / SMA(16,16) , SMB(16,16) , SMD(16,16) , SMG(16) ,
SME(16,16) , SMP(16,16) , SMF(16)
    COMMON /MISC / delt , XX(1001), time
    COMMON /PARS / TON ,XMAX
    common/ints/ n, nj, Numbertimesteps
    ms=2.7
    nu=0.0114 !!!electrolyte volume per cell
    F = 96490.0
    R = 8.3145
    T = 303.15  !Kelvin
    c_rate=0.1
    current=ms*1.675*c_rate !'?
    ar=0.96

    fH=0.924   !gLmol-1
    fM=0.604   !gLmol-1
    fL=0.427   !gLmol-1

    EH0=2.43
```

```
EL0=1.9
EM0=2.41
iH0=5.0
iM0=5.0
iL0=5.0
MS8 = 32.0

nh=4.0
nL=2.0
nm=2.0
ns8=8.0
ns4=4.0
ns2=2.0
ns=1.0



rhos=2000.0 !Density of precipitated Sulfur



Satmass=0.0000001
kp=5000.0  ! s^-1 dissuliton rate
ks=0.0001 !s^-1 shuttle rate

c1=Cprev(1,j)
c2=Cprev(2,j)
c3=Cprev(3,j)
c4=Cprev(4,j)
c5=Cprev(5,j)

! ************* BOUNDARY CONDITIONS********** (BEGINNING)
IF ( J.EQ.1 ) THEN
DO ic = 1 , N
```

```
      dcdx(ic)=(-Cprev(ic,j+2)-3.0*Cprev(ic,j)+4.0*Cprev(ic,j+1))/(2.0*h)
   ENDDO

   SME(1,1)= 1.0/delt+ks
   SME(1,6)=ns8*Ms8/(nh*F)
   SMF(1)= -(ns8*Ms8*Cprev(6,J)/(nh*F))-ks*Cprev(1,J)

   SME(2,1)=-ks
   SME(2,2)= 1.0/delt
   SME(2,6)= -ns8*Ms8/(nh*F)
   SME(2,7)= ns4*MS8/(nm*F)
   SMF(2)=(ns8*Ms8*Cprev(6,J)/(nh*F))+ks*Cprev(1,J)-(ns4*Ms8*Cprev(7,J)/(nm*F))


   SME(3,3)=1.0/delt
   SME(3,7)=-ns4*Ms8/(nm*F)
   SME(3,8)= ns2*Ms8/(nl*F)
   SMF(3)= ns4*MS8*Cprev(7,J)/(nm*F)- ns2*MS8*Cprev(8,J)/(nl*F)


   SME(4,4)= (Cprev(5,J)*kp/(rhos*nu))+1.0/delt
   SME(4,5)= -kp*(Satmass-Cprev(4,J))/(nu*rhos)
   SME(4,8)= -ns2*Ms8/(nl*F)
   SMF(4)= (ns2*MS8*Cprev(8,J)/(nl*F))-(kp*Cprev(5,J)*(Cprev(4,J)-
satmass)/(nu*rhos))

   SME(5,4)= -kp*Cprev(5,J)/(nu*rhos)

   SME(5,5)= -(kp*(Cprev(4,J)-satmass)/(nu*rhos))+1.0/delt

   SMF(5)= kp*Cprev(5,J)*(Cprev(4,J)-satmass)/(nu*rhos)
```

SME(6,6)=-1.0

SME(6,10)= -2.0*iH0*ar*nh*F*(cosh(nh*F*Cprev(10,J)/(2.0*R*T)))/(2.0*R*T)

SMF(6)= Cprev(6,J)+2.0*iH0*ar*sinh(nh*F*Cprev(10,J)/(2.0*R*T))

SME(7,7)=-1.0

SME(7,11)=-2.0*iM0*ar*nm*F*(cosh(nm*F*Cprev(11,J)/(2.0*R*T)))/(2.0*R*T)

SMF(7)=Cprev(7,J)+2.0*iM0*ar*sinh(nm*F*Cprev(11,J)/(2.0*R*T))

SME(8,6)=1.0

SME(8,7)=1.0

SME(8,8)=1.0

SMF(8)=current-Cprev(6,J)-Cprev(7,J)-Cprev(8,J)

SME(9,9)=1.0

SME(9,12)=-1.0

SME(9,15)=-1.0

SMF(9)=-Cprev(9,J)+Cprev(12,J)+Cprev(15,J)

SME(10,9)=-1.0

SME(10,10)=1.0

SME(10,13)=1.0

SMF(10)=-Cprev(10,J)+Cprev(9,J)-Cprev(13,J)

SME(11,9)=-1.0

SME(11,11)=1.0

SME(11,14)=1.0

SMF(11)=-Cprev(11,J)+Cprev(9,J)-Cprev(14,J)

SME(12,8)=-1.0

SME(12,12)= -(iL0*ar*nl*F*(cosh(nl*F*Cprev(12,J)/(2.0*R*T)))/(R*T))

```
SMF(12)=Cprev(8,J)+2.0*iL0*ar*sinh(nl*F*Cprev(12,J)/(2.0*R*T))


SME(13,1)=-R*T/(nH*F*Cprev(1,J))
SME(13,2)=2.0*R*T/(nH*F*Cprev(2,J))
SME(13,13)=1.0
SMF(13)=-Cprev(13,J)+EH0+((R*T)/(nh*F))*(log((fh*Cprev(1,J))/((Cprev(2,J))**2)))

SME(14,2)=-R*T/(nM*F*Cprev(2,J))
SME(14,3)=2.0*R*T/(nM*F*Cprev(3,J))
SME(14,14)=1.0
SMF(14)=-
Cprev(14,J)+EM0+((R*T)/(nm*F))*(log((fm*Cprev(2,J))/((Cprev(3,J))**2)))

SME(15,3)=-R*T/(nl*F*Cprev(3,J))
SME(15,4)=2.0*R*T/(nl*F*Cprev(4,J))
SME(15,15)=1.0
SMF(15)= -Cprev(15,J)+EL0+((R*T)/(nl*F))*(log((fl*Cprev(3,J))/((Cprev(4,J))**2)))

RETURN
ENDIF
!********************* BOUNDARY CONDITIONS ************* (END)
IF ( J.EQ.NJ ) THEN
DO ic = 1 , N
DCDx(ic) = (3.0*CPRev(ic,J)-4.0*CPRev(ic,J-1)+CPRev(ic,J-2))/2.0/H
ENDDO


SME(1,1)= 1.0/delt+ks
SME(1,6)=ns8*Ms8/(nh*F)
SMF(1)= -(ns8*Ms8*Cprev(6,J)/(nh*F))-ks*Cprev(1,J)

SME(2,1)=-ks
```

```
SME(2,2)= 1.0/delt
SME(2,6)= -ns8*Ms8/(nh*F)
SME(2,7)= ns4*MS8/(nm*F)
SMF(2)=(ns8*Ms8*Cprev(6,J)/(nh*F))+ks*Cprev(1,J)-(ns4*Ms8*Cprev(7,J)/(nm*F))


SME(3,3)=1.0/delt
SME(3,7)=-ns4*Ms8/(nm*F)
SME(3,8)= ns2*Ms8/(nl*F)
SMF(3)= ns4*MS8*Cprev(7,J)/(nm*F)- ns2*MS8*Cprev(8,J)/(nl*F)


SME(4,4)= (Cprev(5,J)*kp/(rhos*nu))+1.0/delt
SME(4,5)= -kp*(Satmass-Cprev(4,J))/(nu*rhos)
SME(4,8)= -ns2*Ms8/(nl*F)
SMF(4)= (ns2*MS8*Cprev(8,J)/(nl*F))-(kp*Cprev(5,J)*(Cprev(4,J)-
satmass)/(nu*rhos))

SME(5,4)= -kp*Cprev(5,J)/(nu*rhos)
SME(5,5)= -(kp*(Cprev(4,J)-satmass)/(nu*rhos))+1.0/delt
SMF(5)= kp*Cprev(5,J)*(Cprev(4,J)-satmass)/(nu*rhos)


SME(6,6)=-1.0
SME(6,10)= -2.0*iH0*ar*nh*F*(cosh(nh*F*Cprev(10,J)/(2.0*R*T)))/(2.0*R*T)
SMF(6)= Cprev(6,J)+2.0*iH0*ar*sinh(nh*F*Cprev(10,J)/(2.0*R*T))


SME(7,7)=-1.0
SME(7,11)=-2.0*iM0*ar*nm*F*(cosh(nm*F*Cprev(11,J)/(2.0*R*T)))/(2.0*R*T)
SMF(7)=Cprev(7,J)+2.0*iM0*ar*sinh(nm*F*Cprev(11,J)/(2.0*R*T))

SME(8,6)=1.0
```

```
 SME(8,7)=1.0
 SME(8,8)=1.0
 SMF(8)=current-Cprev(6,J)-Cprev(7,J)-Cprev(8,J)

SME(9,9)=1.0
SME(9,12)=-1.0
SME(9,15)=-1.0
SMF(9)=-Cprev(9,J)+Cprev(12,J)+Cprev(15,J)

 SME(10,9)=-1.0
 SME(10,10)=1.0
SME(10,13)=1.0
SMF(10)=-Cprev(10,J)+Cprev(9,J)-Cprev(13,J)


SME(11,9)=-1.0
SME(11,11)=1.0
SME(11,14)=1.0
SMF(11)=-Cprev(11,J)+Cprev(9,J)-Cprev(14,J)


 SME(12,8)=-1.0
 SME(12,12)= -(iL0*ar*nl*F*(cosh(nl*F*Cprev(12,J)/(2.0*R*T)))/(R*T))
 SMF(12)=Cprev(8,J)+2.0*iL0*ar*sinh(nl*F*Cprev(12,J)/(2.0*R*T))

 SME(13,1)=-R*T/(nH*F*Cprev(1,J))
 SME(13,2)=2.0*R*T/(nH*F*Cprev(2,J))
 SME(13,13)=1.0
 SMF(13)=-Cprev(13,J)+EH0+((R*T)/(nh*F))*(log((fh*Cprev(1,J))/((Cprev(2,J))**2)))

 SME(14,2)=-R*T/(nM*F*Cprev(2,J))
 SME(14,3)=2.0*R*T/(nM*F*Cprev(3,J))
 SME(14,14)=1.0
```

```
   SMF(14)=-
Cprev(14,J)+EM0+((R*T)/(nm*F))*(log((fm*Cprev(2,J))/((Cprev(3,J))**2)))

   SME(15,3)=-R*T/(nl*F*Cprev(3,J))
   SME(15,4)=2.0*R*T/(nl*F*Cprev(4,J))
   SME(15,15)=1.0
   SMF(15)= -Cprev(15,J)+EL0+((R*T)/(nl*F))*(log((fl*Cprev(3,J))/((Cprev(4,J))**2)))

   RETURN
   ENDIF

   ! ************* GOVERNING EQUATIONS AFTER LINERIZATION
**********************

    DO ic = 1 , N
    DCDx(ic) = (CPRev(ic,J+1)-CPRev(ic,J-1))/2.D0/H
    D2Cdx2(ic) = (CPRev(ic,J+1)-2.0*CPRev(ic,J)+CPRev(ic,J-1))/H**2
    ENDDO

    SMD(1,1)= 1.0/delt+ks
    SMD(1,6)=ns8*Ms8/(nh*F)
    SMG(1)= -(ns8*Ms8*Cprev(6,J)/(nh*F))-ks*Cprev(1,J)

    SMD(2,1)=-ks
    SMD(2,2)= 1.0/delt
    SMD(2,6)= -ns8*Ms8/(nh*F)
    SMD(2,7)= ns4*MS8/(nm*F)
    SMG(2)=(ns8*Ms8*Cprev(6,J)/(nh*F))+ks*Cprev(1,J)-(ns4*Ms8*Cprev(7,J)/(nm*F))



    SMD(3,3)=1.0/delt
    SMD(3,7)=-ns4*Ms8/(nm*F)
    SMD(3,8)= ns2*Ms8/(nl*F)
```

```
SMG(3)= ns4*MS8*Cprev(7,J)/(nm*F)- ns2*MS8*Cprev(8,J)/(nl*F)


SMD(4,4)= (Cprev(5,J)*kp/(rhos*nu))+1.0/delt
SMD(4,5)= -kp*(Satmass-Cprev(4,J))/(nu*rhos)
SMD(4,8)= -ns2*Ms8/(nl*F)
SMG(4)= (ns2*MS8*Cprev(8,J)/(nl*F))-(kp*Cprev(5,J)*(Cprev(4,J)-
satmass)/(nu*rhos))

SMD(5,4)= -kp*Cprev(5,J)/(nu*rhos)
SMD(5,5)= -(kp*(Cprev(4,J)-satmass)/(nu*rhos))+1.0/delt
SMG(5)= kp*Cprev(5,J)*(Cprev(4,J)-satmass)/(nu*rhos)


SMD(6,6)=-1.0
SMD(6,10)= -2.0*iH0*ar*nh*F*(cosh(nh*F*Cprev(10,J)/(2.0*R*T)))/(2.0*R*T)
SMG(6)= Cprev(6,J)+2.0*iH0*ar*sinh(nh*F*Cprev(10,J)/(2.0*R*T))


SMD(7,7)=-1.0
SMD(7,11)=-2.0*iM0*ar*nm*F*(cosh(nm*F*Cprev(11,J)/(2.0*R*T)))/(2.0*R*T)
SMG(7)=Cprev(7,J)+2.0*iM0*ar*sinh(nm*F*Cprev(11,J)/(2.0*R*T))

SMD(8,6)=1.0
SMD(8,7)=1.0
SMD(8,8)=1.0
SMG(8)=current-Cprev(6,J)-Cprev(7,J)-Cprev(8,J)

SMD(9,9)=1.0
SMD(9,12)=-1.0
SMD(9,15)=-1.0
SMG(9)=-Cprev(9,J)+Cprev(12,J)+Cprev(15,J)
```

```
 SMD(10,9)=-1.0
 SMD(10,10)=1.0
SMD(10,13)=1.0
SMG(10)=-Cprev(10,J)+Cprev(9,J)-Cprev(13,J)

SMD(11,9)=-1.0
SMD(11,11)=1.0
SMD(11,14)=1.0
SMG(11)=-Cprev(11,J)+Cprev(9,J)-Cprev(14,J)


 SMD(12,8)=-1.0
 SMD(12,12)= -(iL0*ar*nl*F*(cosh(nl*F*Cprev(12,J)/(2.0*R*T)))/(R*T))
 SMG(12)=Cprev(8,J)+2.0*iL0*ar*sinh(nl*F*Cprev(12,J)/(2.0*R*T))



 SMD(13,1)=-R*T/(nH*F*Cprev(1,J))
 SMD(13,2)=2.0*R*T/(nH*F*Cprev(2,J))
 SMD(13,13)=1.0
 SMG(13)=-Cprev(13,J)+EH0+((R*T)/(nh*F))*(log((fh*Cprev(1,J))/((Cprev(2,J))**2)))

 SMD(14,2)=-R*T/(nM*F*Cprev(2,J))
 SMD(14,3)=2.0*R*T/(nM*F*Cprev(3,J))
 SMD(14,14)=1.0
 SMG(14)=
Cprev(14,J)+EM0+((R*T)/(nm*F))*(log((fm*Cprev(2,J))/((Cprev(3,J))**2)))

 SMD(15,3)=-R*T/(nl*F*Cprev(3,J))
 SMD(15,4)=2.0*R*T/(nl*F*Cprev(4,J))
 SMD(15,15)=1.0
 SMG(15)= -Cprev(15,J)+EL0+((R*T)/(nl*F))*(log((fl*Cprev(3,J))/((Cprev(4,J))**2)))
```

```
   END
   SUBROUTINE ABDGXY(H,J)
    IMPLICIT NONE
    !*--ABDGXY178
    !*** Start of declarations inserted by SPAG
    DOUBLE PRECISION A , B , CPRev , D , D2Cdx2 , DCDx , delc , G , SMA , SMB ,
&
       & SMD , SME , SMF , SMG , SMP , X ,Y, kp, delt,time,ton, xx, h, xmax
    INTEGER ii , J , kk , N , NJ, Numbertimesteps
       !*** End of declarations inserted by SPAG
    COMMON A(15,15) , B(15,15) , DELc(15,903) , D(15,31) , G(15) , X(15,15) , &
       & Y(15,15)
       !COMMON /TEST / CPRev(12,903) , DCDx(12) , D2Cdx2(12)
    COMMON /SMALL / SMA(16,16) , SMB(16,16) , SMD(16,16) , SMG(16) , &
       & SME(16,16) , SMP(16,16) , SMF(16)
    COMMON /var /  CPRev(15,903) , DCDx(15) , D2Cdx2(15), kp
    common/misc/ xx(1001), delt, time
    common/pars/ ton, xmax
    common/ints/ n, nj, Numbertimesteps

    IF ( J.EQ.1 ) THEN
    DO ii = 1 , N
    DO kk = 1 , N
       B(ii,kk) = H*SME(ii,kk) - 1.5*SMP(ii,kk)
       D(ii,kk) = 2.0*SMP(ii,kk)
       X(ii,kk) = -0.5*SMP(ii,kk)
    ENDDO
       G(ii) = H*SMF(ii)
    ENDDO
    RETURN
    ENDIF
    IF ( J.EQ.NJ ) THEN
```

```
DO ii = 1 , N
DO kk = 1 , N
   B(ii,kk) = H*SME(ii,kk) + 1.5*SMP(ii,kk)
   A(ii,kk) = -2.0*SMP(ii,kk)
   Y(ii,kk) = 0.5*SMP(ii,kk)
ENDDO
   G(ii) = H*SMF(ii)
ENDDO
RETURN
ENDIF
DO ii = 1 , N
DO kk = 1 , N
   A(ii,kk) = SMA(ii,kk) - H/2.0*SMB(ii,kk)
   B(ii,kk) = -2.0*SMA(ii,kk) + H**2*SMD(ii,kk)
   D(ii,kk) = SMA(ii,kk) + H/2.0*SMB(ii,kk)
ENDDO
   G(ii) = H**2*SMG(ii)
ENDDO
END

   !*******************

   SUBROUTINE BOUND_VAL(H)
   IMPLICIT NONE

   !*** Start of declarations inserted by SPAG
   DOUBLE PRECISION A , B , CPRev , D , D2Cdx2 , DCDx , delc , G , &
   & H , SMA , SMB , SMD , SME , SMF , SMG , SMP , X ,&
   & Y, kp,xx,delt,time,ton,xmax
   INTEGER ic , j , k , kc , N , NJ, Numbertimesteps
   !*** End of declarations inserted by SPAG
   COMMON A(15,15) , B(15,15) , DELc(15,903) , D(15,31) , G(15) , X(15,15) , &
   & Y(15,15)
```

```
COMMON /SMALL / SMA(16,16) , SMB(16,16) , SMD(16,16) , SMG(16) , &
& SME(16,16) , SMP(16,16) , SMF(16)
COMMON /var /  CPRev(15,903) , DCDx(15) , D2Cdx2(15), kp
common/misc/ xx(1001), delt, time
common/pars/ ton, xmax
common/ints/ n, nj, Numbertimesteps
!_____________________
! This subroutine assumes solution of a linear boundary-value problem at
! a given time step. There is thus no need for iteration.
!_____________________________
DO j = 1 , NJ
DO ic = 1 , N
DO kc = 1 , N
SMA(ic,kc) = 0.0
SMB(ic,kc) = 0.0
SMD(ic,kc) = 0.0
SMP(ic,kc) = 0.0
SME(ic,kc) = 0.0
ENDDO
ENDDO
CALL FILLMAT(H,j)
CALL ABDGXY(H,j)
CALL BAND(j)
ENDDO

DO k = 1 , N
DO j = 1 , NJ
CPRev(k,j) = CPRev(k,j) + delc(k,j)
ENDDO
ENDDO
END
```

```
!*************************************

      SUBROUTINE MATINV(N,M,Determ)
      IMPLICIT NONE
      !*--MATINV266
      !*** Start of declarations inserted by SPAG
      DOUBLE PRECISION A , B , bmax , bnext , btry , D , DELc , Determ ,&
      & f , save, G,x,y
      INTEGER i , id , irow , j , jc , jcol , k , M , N , nn
      !*** End of declarations inserted by SPAG
      DIMENSION id(15)

      COMMON A(15,15) , B(15,15) , delc(15,903) , D(15,31), G(15), X(15,15),
Y(15,15)
      Determ = 1.0
      DO i = 1 , N
      id(i) = 0
      ENDDO
      DO nn = 1 , N
      bmax = 1.1
      DO i = 1 , N
      IF ( id(i).EQ.0 ) THEN
      bnext = 0.0
      btry = 0.0
      DO j = 1 , N
      IF ( id(j).EQ.0 ) THEN
      IF ( DABS(B(i,j)).GT.bnext ) THEN
      bnext = DABS(B(i,j))
      IF ( bnext.GT.btry ) THEN
      bnext = btry
      btry = DABS(B(i,j))
```

```
jc = j
ENDIF
ENDIF
ENDIF
ENDDO
IF ( bnext.LT.bmax*btry ) THEN
bmax = bnext/btry
irow = i
jcol = jc
ENDIF
ENDIF
ENDDO
IF ( id(jc).EQ.0 ) THEN
id(jcol) = 1
IF ( jcol.NE.irow ) THEN
DO j = 1 , N
save = B(irow,j)
B(irow,j) = B(jcol,j)
B(jcol,j) = save
ENDDO
DO k = 1 , M
save = D(irow,k)
D(irow,k) = D(jcol,k)
D(jcol,k) = save
ENDDO
ENDIF
f = 1.0/B(jcol,jcol)
DO j = 1 , N
B(jcol,j) = B(jcol,j)*f
ENDDO
DO k = 1 , M
D(jcol,k) = D(jcol,k)*f
ENDDO
```

```
      DO i = 1 , N
      IF ( i.NE.jcol ) THEN
      f = B(i,jcol)
      DO j = 1 , N
      B(i,j) = B(i,j) - f*B(jcol,j)
      ENDDO
      DO k = 1 , M
      D(i,k) = D(i,k) - f*D(jcol,k)
      ENDDO
      ENDIF
      ENDDO
      ELSE
      Determ = 0.0
      RETURN
      ENDIF
      ENDDO
      END
      !*************************************************************

      SUBROUTINE BAND(J)
      IMPLICIT NONE
      !*--BAND345
      !*** Start of declarations inserted by SPAG
      DOUBLE PRECISION A , B , D , DELc , determ , e , G , X , Y
      INTEGER i , J , jj , k , l , lpn , m , N , NJ , np1,Numbertimesteps
      !*** End of declarations inserted by SPAG
      DIMENSION e(15,16,903)
      COMMON A(15,15) , B(15,15) , DELc(15,903) , D(15,31) , G(15) , X(15,15) ,
Y(15,15)
      common/ints/ n, nj, Numbertimesteps
      SAVE e , np1
      IF ( J.LT.2 ) THEN
      np1 = N + 1
```

```
DO i = 1 , N
D(i,2*N+1) = G(i)
DO l = 1 , N
lpn = l + N
D(i,lpn) = X(i,l)
ENDDO
ENDDO
CALL MATINV(N,2*N+1,determ)
IF ( determ.EQ.0 ) PRINT 99001 , J
DO k = 1 , N
e(k,np1,1) = D(k,2*N+1)
DO l = 1 , N
e(k,l,1) = -D(k,l)
lpn = l + N
X(k,l) = -D(k,lpn)
ENDDO
ENDDO
RETURN
ELSEIF ( J.EQ.2 ) THEN
DO i = 1 , N
DO k = 1 , N
DO l = 1 , N
D(i,k) = D(i,k) + A(i,l)*X(l,k)
ENDDO
ENDDO
ENDDO
ENDIF
IF ( J.GE.NJ ) THEN
DO i = 1 , N
DO l = 1 , N
G(i) = G(i) - Y(i,l)*e(l,np1,J-2)
DO m = 1 , N
A(i,l) = A(i,l) + Y(i,m)*e(m,l,J-2)
```

```
ENDDO
ENDDO
ENDDO
ENDIF
DO i = 1 , N
D(i,np1) = -G(i)
DO l = 1 , N
D(i,np1) = D(i,np1) + A(i,l)*e(l,np1,J-1)
DO k = 1 , N
B(i,k) = B(i,k) + A(i,l)*e(l,k,J-1)
ENDDO
ENDDO
ENDDO
CALL MATINV(N,np1,determ)
IF ( determ.EQ.0 ) PRINT 99001 , J
DO k = 1 , N
DO m = 1 , np1
e(k,m,J) = -D(k,m)
ENDDO
ENDDO
IF ( J.GE.NJ ) THEN
DO k = 1 , N
delc(k,J) = e(k,np1,J)
ENDDO
DO jj = 2 , NJ
m = NJ - jj + 1
DO k = 1 , N
delc(k,m) = e(k,np1,m)
DO l = 1 , N
delc(k,m) = DELc(k,m) + e(k,l,m)*delc(l,m+1)
ENDDO
ENDDO
ENDDO
```

```
DO l = 1 , N
DO k = 1 , N
delc(k,1) = delc(k,1) + X(k,l)*delc(l,3)
ENDDO
ENDDO
ENDIF
99001 FORMAT (' DETERM=0 AT J=',I4)
END
```

APPENDIX B: FORTRAN CODE FOR CHARGE PROCESS

```
      implicit none
      DOUBLE PRECISION A , B , CPRev  , D , D2Cdx2 , DCDx , SMA, SMB, SMD,
SMG, SME, SMP,SMF, &
      & delc , delt , G , h , time ,c1 , c2 , c3 , c4 , c5 , c6 , c7 ,c8 ,c9, c10 , c11, c12,c13,
c14,c15 ,&
      & TON , X , XX , Y, S8in, S4in , S2in, S_in, ms , current, &
      & R, F, T, kp, ar, fh, fm,fl, iM0, EM0, nh, nm, nl, ns8, ns4 , ns2, ns, XMAx
      INTEGER it ,i, j , N , NJ , Numbertimesteps

      COMMON A(15,15) , B(15,15) , DELc(15,903) , D(15,31) , G(15) , X(15,15) ,
Y(15,15)

      COMMON/small/  SMA(16,16) , SMB(16,16) , SMD(16,16) , SMG(16) , &
      & SME(16,16) , SMP(16,16) , SMF(16)

      COMMON /var / CPRev(15,903) , DCDx(15) , D2Cdx2(15) , kp
      COMMON /misc/ xx(1001), delt, time
      COMMON /pars/ ton, xmax
      COMMON /ints/ n, nj, Numbertimesteps


      OPEN (70,FILE='ref-charge-01C-1.txt',STATUS='unknown')
      OPEN (73,FILE='ref-charge-01C-2.txt',STATUS='unknown')
      OPEN (71, FILE='ref-charge-01C-capacityandvoltage.txt',STATUS='unknown')
        time=0.0
        delt= 0.1
        CALL READ_DATA(h)
        CALL INTIAL_CONDITION(h)
        DO it = 1 , NUMbertimesteps
        CALL BOUND_VAL(h)
        time = time + delt
```

```
DO j = 1 , NJ
c1=Cprev(1,j)
c2=Cprev(2,j)
c3=Cprev(3,j)
c4=Cprev(4,j)
c5=Cprev(5,j)
c6=Cprev(6,j)
c7=Cprev(7,j)
c8=Cprev(8,j)
c9=Cprev(9,j)
c10=Cprev(10,j)
c11=Cprev(11,j)
c12=Cprev(12,j)
c13=Cprev(13,j)
c14=Cprev(14,j)
c15=Cprev(15,j)

! concentration of species cannot be lower than zero
  if (c1.lt.0.0) then
  c1=1.0E-40
  Cprev(1,j)=c1
end if

  if (c2.lt.0.0) then
    c2=1.0E-40
  cprev(2,j)=c2
end if

  if (c3.lt.0.0) then
  c3=1.0E-40
  cprev(3,j)=c3
end if
```

```
    if (c4.lt.0.0) then
      c4=1.0E-40
      cprev(4,j)=c4
 end if

    if (c5.lt.0.0) then
    c5=1.0E-40
    cprev(5,j)=c5
end if



    if (c1.gt.2.7) then
    c1=2.7
    cprev(1,j)=c1
end if

    if (c2.gt.2.7) then
    c2=2.7
    cprev(2,j)=c2
end if

    if (c3.gt.2.7) then
    c3=2.7
    cprev(3,j)=c3
end if
    if (c4.gt.2.7) then
    c4=2.7
    cprev(4,j)=c4
end if
    if (c5.gt.2.7) then
    c5=2.7
```

```
   cprev(5,j)=c5
 end if

END DO


   DO j = 1 , nj
   if (j.eq.nj) then

write(70,910)time,xx(j),cprev(1,j),cprev(2,j),cprev(3,j),&
&cprev(4,j),cprev(5,j),cprev(6,j),cprev(7,j), cprev(8,j),&
&cprev(9,j)
910 FORMAT (11(G12.6,1X))
write(73,913)time,xx(j),cprev(10,j), cprev(11,j),cprev(12,j),cprev(13,j),&
&cprev(14,j),cprev(15,j)
913 FORMAT (8(G12.6,1X))
WRITE (71,911)(1675.0/(3600.0/0.1))*(time), cprev(9,j)
911 FORMAT (2(G12.6,1X))
 end if
END DO
END DO
END
!************************************************
! USER SPECIFIES


SUBROUTINE READ_DATA(H)
IMPLICIT NONE
!*--READ_DATA54
!*** Start of declarations inserted by SPAG
DOUBLE PRECISION A , B , CPRev , D , D2Cdx2 , DCDx , Delc , Delt , G , H  ,
TON , X , &
& XMAx , XX , Y , ms, R , F , T, kp,time,&
```

```
& SMA, SMB, SMD, SMG, SME, SMP, SMF,  fh, fm,fl, iM0, EM0
INTEGER j , N , NJ , Numbertimesteps
!*** End of declarations inserted by SPAG
COMMON A(15,15) , B(15,15) , DELc(15,903) , D(15,31) , G(15) , X(15,15) , &
& Y(15,15)
COMMON /SMALL / SMA(16,16) , SMB(16,16) , SMD(16,16) , SMG(16) , &
& SME(16,16) , SMP(16,16) , SMF(16)
!COMMON /TEST / CPRev(15,903) , DCDx(15) , D2Cdx2(15)
COMMON /var / CPRev(15,903) , DCDx(15) , D2Cdx2(15), kp
COMMON /MISC / DELt , XX(1001), time
COMMON /PARS / TON , XMAx
common/ints/ n, nj, Numbertimesteps



N=15
NJ=401
Numbertimesteps= 36000*100
TON= 36000
XMAx=1.0

!_____________________________
! N is the number of unknown
! NJ is the number of node points
! xmax is the length of the domain
! Ton is the duration of the simulation
!_____________________________________________



DELt = TON/FLOAT(Numbertimesteps)
```

```
H = XMAx/FLOAT(NJ-1)
DO j = 1 , NJ
XX(j) = H*FLOAT(j-1)
if(j.eq.NJ) then
   XX(j)=xmax
end if
ENDDO
END

! **********  INITIAL CONDITIONS ********
!_____________________

SUBROUTINE INTIAL_CONDITION(H)
IMPLICIT NONE
!*--INTIAL_CONDITION91
!*** Start of declarations inserted by SPAG
DOUBLE PRECISION A , B , CPRev , D , D2Cdx2 , DCDx , Delc , G ,kp,xx,delt,
time,ton,xmax, &
& H , X , Y , S8in, S4in , S2in, S_in, Spin, IHin, ILin, Vin , current, nH, nM, nL,&
& F, R, T, ms, SMA, SMB, SMD, SMG, SME, SMP, SMF, ar, fh, fm,fl, iH0,
iL0,iM0, EM0, EL0, EH0
INTEGER j , N , NJ, i,Numbertimesteps
!*** End of declarations inserted by SPAG
COMMON A(15,15) , B(15,15) , DELc(15,903) , D(15,31) , G(15) , X(15,15) , &
& Y(15,15)
COMMON /SMALL / SMA(16,16) , SMB(16,16) , SMD(16,16) , SMG(16) , &
& SME(16,16) , SMP(16,16) , SMF(16)

COMMON /var / CPRev(15,903) , DCDx(15) , D2Cdx2(15), kp
common/misc/ xx(1001), delt, time
common/pars/ ton, xmax
common/ints/ n, nj, Numbertimesteps
```

```
ms=2.7
F = 96490! f
R = 8.3145 !JK-1mol-1
T = 303.15 !Kelvin
ar=0.96 !m2
current =-ms*1.675*0.1
fH=0.924   !gLmol-1
fM=0.604   !gLmol-1
fL=0.427   !gLmol-1
EH0=2.43      !Volt
EM0= 2.41     !Volt
EL0=1.9       !Volt
iH0=5.0       !Am-2
iM0=5.0       !Am-2
iL0=5.0       !Am-2
! nH=4.0
!nL=2.0
! nM=2.0



DO j = 1 , nj
CPRev(1,j) = 0.354675E-26
CPRev(6,j) = 0.0
CPRev(7,j) = 0.0
CPRev(8,j) = current
CPRev(9,j) = 2.0
CPRev(10,j) = 0.0
CPRev(11,j) = 0.0
CPRev(12,j) = (asinh(-CPRev(8,j)/(2.0*iL0*ar)))*(2.0*R*T/(2.0*F))
CPRev(13,j) = CPRev(9,j) - CPRev(10,j)
CPRev(14,j) = CPRev(9,j)- CPRev(11,j)
CPRev(15,j) = CPRev(9,j) - CPRev(12,j)
```

```
CPRev(2,j) =0.736822E-7
CPRev(3,j) =0.111301
CPRev(4,j) = 0.364197E-06
CPRev(5,j) = 2.58871



IF ( j.EQ.1 ) THEN
do i= 1 , 15
print*, CPRev(i,j)
ENDDO
ENDIF
ENDDO
END



SUBROUTINE FILLMAT(H,J)
IMPLICIT NONE
!*--FILLMAT117

DOUBLE PRECISION A , B , CPRev  , D , D2Cdx2 , DCDx , &
& DELc , delt , G , H , SMA , SMB , SMD , SME , SMF , SMG , SMP , ks , MS8 ,
&
& c1,c2,c3,c4,c5,c6, c7, c8, c9, c10, c11, c12, c13, c14, c15, &
& NA , ne , ns8 , ns4 , ns2 , ns , R , rhos , &
& fh , fl , v , ms , EH0 , EL0 , iH0 , iL0 , Satmass, &
& kp , S8in, S4in , S2in, S_in, Spin, IHin, ILin, Vin, &
& current,  F, T , time, ar,  fm, iM0, EM0, nH, nM, nL , nu

DOUBLE PRECISION TON , X , XMAx , XX , Y
INTEGER ic , J , N , NJ , Numbertimesteps , i
```

```
      COMMON A(15,15) , B(15,15) , DELc(15,903) , D(15,31) , G(15) , X(15,15) ,
Y(15,15)
      COMMON /var / CPRev(15,903) , DCDx(15) , D2Cdx2(15), kp
      COMMON /SMALL / SMA(16,16) , SMB(16,16) , SMD(16,16) , SMG(16) ,
SME(16,16) , SMP(16,16) , SMF(16)
      COMMON /MISC / delt , XX(1001), time
      COMMON /PARS / TON ,XMAX
      common/ints/ n, nj, Numbertimesteps
      ms=2.7
      nu=0.0114
      F = 96490.0
      R = 8.3145
      T = 303.15  !Kelvin
      current=-ms*1.675*0.1 !'?
      ar=0.96

      fH=0.924   !gLmol-1
      fM=0.604   !gLmol-1
      fL=0.427   !gLmol-1

      EH0=2.43
      EL0=1.9
      EM0=2.41
      iH0=5.0
      iM0=5.0
      iL0=5.0
      MS8 = 32.0

      nH=4.0
      nL=2.0
      nM=2.0
```

```
ns8=8.0
ns4=4.0
ns2=2.0
ns=1.0


rhos=2000.0
ar=0.96



Satmass=0.0000001
kp=5000.0  ! s^-1 dissuliton rate
ks=0.0001 !s^-1 shuttle rate

c1=Cprev(1,j)
c2=Cprev(2,j)
c3=Cprev(3,j)
c4=Cprev(4,j)
c5=Cprev(5,j)

! ************* BOUNDARY CONDITIONS********** (BEGINNING)
IF ( J.EQ.1 ) THEN
DO ic = 1 , N
   dcdx(ic)=(-Cprev(ic,j+2)-3.0*Cprev(ic,j)+4.0*Cprev(ic,j+1))/(2.0*h)
ENDDO

SME(1,1)= 1.0/delt+ks
SME(1,6)=ns8*Ms8/(nh*F)
SMF(1)= -(ns8*Ms8*Cprev(6,J)/(nh*F))-ks*Cprev(1,J)

SME(2,1)=-ks
SME(2,2)= 1.0/delt
```

```
SME(2,6)= -ns8*Ms8/(nh*F)
SME(2,7)= ns4*MS8/(nm*F)
SMF(2)=(ns8*Ms8*Cprev(6,J)/(nh*F))+ks*Cprev(1,J)-
(ns4*Ms8*Cprev(7,J)/(nm*F))

SME(3,3)=1.0/delt
SME(3,7)=-ns4*Ms8/(nm*F)
SME(3,8)= ns2*Ms8/(nl*F)
SMF(3)= ns4*MS8*Cprev(7,J)/(nm*F)- ns2*MS8*Cprev(8,J)/(nl*F)

SME(4,4)= (Cprev(5,J)*kp/(rhos*nu))+1.0/delt
SME(4,5)= -kp*(Satmass-Cprev(4,J))/(nu*rhos)
SME(4,8)= -ns2*Ms8/(nl*F)
SMF(4)=          (ns2*MS8*Cprev(8,J)/(nl*F))-(kp*Cprev(5,J)*(Cprev(4,J)-
satmass)/(nu*rhos))

SME(5,4)= -kp*Cprev(5,J)/(nu*rhos)

SME(5,5)= -(kp*(Cprev(4,J)-satmass)/(nu*rhos))+1.0/delt

SMF(5)= kp*Cprev(5,J)*(Cprev(4,J)-satmass)/(nu*rhos)

SME(6,6)=-1.0
SME(6,10)= -2.0*iH0*ar*nh*F*(cosh(nh*F*Cprev(10,J)/(2.0*R*T)))/(2.0*R*T)
SMF(6)= Cprev(6,J)+2.0*iH0*ar*sinh(nh*F*Cprev(10,J)/(2.0*R*T))

SME(7,7)=-1.0
SME(7,11)=-2.0*iM0*ar*nm*F*(cosh(nm*F*Cprev(11,J)/(2.0*R*T)))/(2.0*R*T)
SMF(7)=Cprev(7,J)+2.0*iM0*ar*sinh(nm*F*Cprev(11,J)/(2.0*R*T))
```

```
SME(8,6)=1.0
SME(8,7)=1.0
SME(8,8)=1.0
SMF(8)=current-Cprev(6,J)-Cprev(7,J)-Cprev(8,J)

SME(9,9)=1.0
SME(9,12)=-1.0
SME(9,15)=-1.0
SMF(9)=-Cprev(9,J)+Cprev(12,J)+Cprev(15,J)

SME(10,9)=-1.0
SME(10,10)=1.0
SME(10,13)=1.0
SMF(10)=-Cprev(10,J)+Cprev(9,J)-Cprev(13,J)

SME(11,9)=-1.0
SME(11,11)=1.0
SME(11,14)=1.0
SMF(11)=-Cprev(11,J)+Cprev(9,J)-Cprev(14,J)

SME(12,8)=-1.0
SME(12,12)= -(iL0*ar*nl*F*(cosh(nl*F*Cprev(12,J)/(2.0*R*T)))/(R*T))
SMF(12)=Cprev(8,J)+2.0*iL0*ar*sinh(nl*F*Cprev(12,J)/(2.0*R*T))

SME(13,1)=-R*T/(nH*F*Cprev(1,J))
SME(13,2)=2.0*R*T/(nH*F*Cprev(2,J))
SME(13,13)=1.0
SMF(13)=-
Cprev(13,J)+EH0+((R*T)/(nh*F))*(log((fh*Cprev(1,J))/((Cprev(2,J))**2)))
```

```
        SME(14,2)=-R*T/(nM*F*Cprev(2,J))
        SME(14,3)=2.0*R*T/(nM*F*Cprev(3,J))
        SME(14,14)=1.0
        SMF(14)=-
Cprev(14,J)+EM0+((R*T)/(nm*F))*(log((fm*Cprev(2,J))/((Cprev(3,J))**2)))

        SME(15,3)=-R*T/(nl*F*Cprev(3,J))
        SME(15,4)=2.0*R*T/(nl*F*Cprev(4,J))
        SME(15,15)=1.0
        SMF(15)=                                                    -
Cprev(15,J)+EL0+((R*T)/(nl*F))*(log((fl*Cprev(3,J))/((Cprev(4,J))**2)))

        RETURN
        ENDIF
        !********************* BOUNDARY CONDITIONS ************* (END)
        IF ( J.EQ.NJ ) THEN
        DO ic = 1 , N
        DCDx(ic) = (3.0*CPRev(ic,J)-4.0*CPRev(ic,J-1)+CPRev(ic,J-2))/2.0/H
        ENDDO


        SME(1,1)= 1.0/delt+ks
        SME(1,6)=ns8*Ms8/(nh*F)
        SMF(1)= -(ns8*Ms8*Cprev(6,J)/(nh*F))-ks*Cprev(1,J)

        SME(2,1)=-ks
        SME(2,2)= 1.0/delt
        SME(2,6)= -ns8*Ms8/(nh*F)
        SME(2,7)= ns4*MS8/(nm*F)
        SMF(2)=(ns8*Ms8*Cprev(6,J)/(nh*F))+ks*Cprev(1,J)-
(ns4*Ms8*Cprev(7,J)/(nm*F))
```

```
SME(3,3)=1.0/delt
SME(3,7)=-ns4*Ms8/(nm*F)
SME(3,8)= ns2*Ms8/(nl*F)
SMF(3)= ns4*MS8*Cprev(7,J)/(nm*F)- ns2*MS8*Cprev(8,J)/(nl*F)


SME(4,4)= (Cprev(5,J)*kp/(rhos*nu))+1.0/delt
SME(4,5)= -kp*(Satmass-Cprev(4,J))/(nu*rhos)
SME(4,8)= -ns2*Ms8/(nl*F)
SMF(4)=                (ns2*MS8*Cprev(8,J)/(nl*F))-(kp*Cprev(5,J)*(Cprev(4,J)-
satmass)/(nu*rhos))

SME(5,4)= -kp*Cprev(5,J)/(nu*rhos)
SME(5,5)= -(kp*(Cprev(4,J)-satmass)/(nu*rhos))+1.0/delt
SMF(5)= kp*Cprev(5,J)*(Cprev(4,J)-satmass)/(nu*rhos)


SME(6,6)=-1.0
SME(6,10)= -2.0*iH0*ar*nh*F*(cosh(nh*F*Cprev(10,J)/(2.0*R*T)))/(2.0*R*T)
SMF(6)= Cprev(6,J)+2.0*iH0*ar*sinh(nh*F*Cprev(10,J)/(2.0*R*T))


SME(7,7)=-1.0
SME(7,11)=-2.0*iM0*ar*nm*F*(cosh(nm*F*Cprev(11,J)/(2.0*R*T)))/(2.0*R*T)
SMF(7)=Cprev(7,J)+2.0*iM0*ar*sinh(nm*F*Cprev(11,J)/(2.0*R*T))

SME(8,6)=1.0
SME(8,7)=1.0
SME(8,8)=1.0
SMF(8)=current-Cprev(6,J)-Cprev(7,J)-Cprev(8,J)

SME(9,9)=1.0
```

```
SME(9,12)=-1.0
SME(9,15)=-1.0
SMF(9)=-Cprev(9,J)+Cprev(12,J)+Cprev(15,J)

 SME(10,9)=-1.0
 SME(10,10)=1.0
SME(10,13)=1.0
SMF(10)=-Cprev(10,J)+Cprev(9,J)-Cprev(13,J)


SME(11,9)=-1.0
SME(11,11)=1.0
SME(11,14)=1.0
SMF(11)=-Cprev(11,J)+Cprev(9,J)-Cprev(14,J)


 SME(12,8)=-1.0
 SME(12,12)= -(iL0*ar*nl*F*(cosh(nl*F*Cprev(12,J)/(2.0*R*T)))/(R*T))
 SMF(12)=Cprev(8,J)+2.0*iL0*ar*sinh(nl*F*Cprev(12,J)/(2.0*R*T))

 SME(13,1)=-R*T/(nH*F*Cprev(1,J))
 SME(13,2)=2.0*R*T/(nH*F*Cprev(2,J))
 SME(13,13)=1.0
 SMF(13)=-
Cprev(13,J)+EH0+((R*T)/(nh*F))*(log((fh*Cprev(1,J))/((Cprev(2,J))**2)))

 SME(14,2)=-R*T/(nM*F*Cprev(2,J))
 SME(14,3)=2.0*R*T/(nM*F*Cprev(3,J))
 SME(14,14)=1.0
 SMF(14)=-
Cprev(14,J)+EM0+((R*T)/(nm*F))*(log((fm*Cprev(2,J))/((Cprev(3,J))**2)))

 SME(15,3)=-R*T/(nl*F*Cprev(3,J))
```

```
        SME(15,4)=2.0*R*T/(nl*F*Cprev(4,J))
        SME(15,15)=1.0
        SMF(15)=                                                    -
Cprev(15,J)+EL0+((R*T)/(nl*F))*(log((fl*Cprev(3,J))/((Cprev(4,J))**2)))

        RETURN
        ENDIF

        ! ************* GOVERNING EQUATIONS AFTER LINERIZATION
**********************

        DO ic = 1 , N
        DCDx(ic) = (CPRev(ic,J+1)-CPRev(ic,J-1))/2.D0/H
        D2Cdx2(ic) = (CPRev(ic,J+1)-2.0*CPRev(ic,J)+CPRev(ic,J-1))/H**2
        ENDDO

        SMD(1,1)= 1.0/delt+ks
        SMD(1,6)=ns8*Ms8/(nh*F)
        SMG(1)= -(ns8*Ms8*Cprev(6,J)/(nh*F))-ks*Cprev(1,J)

        SMD(2,1)=-ks
        SMD(2,2)= 1.0/delt
        SMD(2,6)= -ns8*Ms8/(nh*F)
        SMD(2,7)= ns4*MS8/(nm*F)
        SMG(2)=(ns8*Ms8*Cprev(6,J)/(nh*F))+ks*Cprev(1,J)-
(ns4*Ms8*Cprev(7,J)/(nm*F))


        SMD(3,3)=1.0/delt
        SMD(3,7)=-ns4*Ms8/(nm*F)
        SMD(3,8)= ns2*Ms8/(nl*F)
        SMG(3)= ns4*MS8*Cprev(7,J)/(nm*F)- ns2*MS8*Cprev(8,J)/(nl*F)
```

```
SMD(4,4)= (Cprev(5,J)*kp/(rhos*nu))+1.0/delt
SMD(4,5)= -kp*(Satmass-Cprev(4,J))/(nu*rhos)
SMD(4,8)= -ns2*Ms8/(nl*F)
SMG(4)=          (ns2*MS8*Cprev(8,J)/(nl*F))-(kp*Cprev(5,J)*(Cprev(4,J)-
satmass)/(nu*rhos))

SMD(5,4)= -kp*Cprev(5,J)/(nu*rhos)
SMD(5,5)= -(kp*(Cprev(4,J)-satmass)/(nu*rhos))+1.0/delt
SMG(5)= kp*Cprev(5,J)*(Cprev(4,J)-satmass)/(nu*rhos)


SMD(6,6)=-1.0
SMD(6,10)= -2.0*iH0*ar*nh*F*(cosh(nh*F*Cprev(10,J)/(2.0*R*T)))/(2.0*R*T)
SMG(6)= Cprev(6,J)+2.0*iH0*ar*sinh(nh*F*Cprev(10,J)/(2.0*R*T))


SMD(7,7)=-1.0
SMD(7,11)=-
2.0*iM0*ar*nm*F*(cosh(nm*F*Cprev(11,J)/(2.0*R*T)))/(2.0*R*T)
SMG(7)=Cprev(7,J)+2.0*iM0*ar*sinh(nm*F*Cprev(11,J)/(2.0*R*T))

SMD(8,6)=1.0
SMD(8,7)=1.0
SMD(8,8)=1.0
SMG(8)=current-Cprev(6,J)-Cprev(7,J)-Cprev(8,J)

SMD(9,9)=1.0
SMD(9,12)=-1.0
SMD(9,15)=-1.0
SMG(9)=-Cprev(9,J)+Cprev(12,J)+Cprev(15,J)

SMD(10,9)=-1.0
```

```
SMD(10,10)=1.0
SMD(10,13)=1.0
SMG(10)=-Cprev(10,J)+Cprev(9,J)-Cprev(13,J)

SMD(11,9)=-1.0
SMD(11,11)=1.0
SMD(11,14)=1.0
SMG(11)=-Cprev(11,J)+Cprev(9,J)-Cprev(14,J)


SMD(12,8)=-1.0
SMD(12,12)= -(iL0*ar*nl*F*(cosh(nl*F*Cprev(12,J)/(2.0*R*T)))/(R*T))
SMG(12)=Cprev(8,J)+2.0*iL0*ar*sinh(nl*F*Cprev(12,J)/(2.0*R*T))


SMD(13,1)=-R*T/(nH*F*Cprev(1,J))
SMD(13,2)=2.0*R*T/(nH*F*Cprev(2,J))
SMD(13,13)=1.0
SMG(13)=-
Cprev(13,J)+EH0+((R*T)/(nh*F))*(log((fh*Cprev(1,J))/((Cprev(2,J))**2)))

SMD(14,2)=-R*T/(nM*F*Cprev(2,J))
SMD(14,3)=2.0*R*T/(nM*F*Cprev(3,J))
SMD(14,14)=1.0
SMG(14)=-
Cprev(14,J)+EM0+((R*T)/(nm*F))*(log((fm*Cprev(2,J))/((Cprev(3,J))**2)))

SMD(15,3)=-R*T/(nl*F*Cprev(3,J))
SMD(15,4)=2.0*R*T/(nl*F*Cprev(4,J))
SMD(15,15)=1.0
SMG(15)=                                                    -
Cprev(15,J)+EL0+((R*T)/(nl*F))*(log((fl*Cprev(3,J))/((Cprev(4,J))**2)))
```

```
      END
      SUBROUTINE ABDGXY(H,J)
       IMPLICIT NONE
       !*--ABDGXY178
       !*** Start of declarations inserted by SPAG
       DOUBLE PRECISION A , B , CPRev , D , D2Cdx2 , DCDx , delc , G , SMA ,
SMB , &
          & SMD , SME , SMF , SMG , SMP , X ,Y, kp, delt,time,ton, xx, h, xmax
       INTEGER ii , J , kk , N , NJ, Numbertimesteps
          !*** End of declarations inserted by SPAG
       COMMON A(15,15) , B(15,15) , DELc(15,903) , D(15,31) , G(15) , X(15,15) , &
          & Y(15,15)
          !COMMON /TEST / CPRev(12,903) , DCDx(12) , D2Cdx2(12)
       COMMON /SMALL / SMA(16,16) , SMB(16,16) , SMD(16,16) , SMG(16) , &
          & SME(16,16) , SMP(16,16) , SMF(16)
       COMMON /var /  CPRev(15,903) , DCDx(15) , D2Cdx2(15), kp
       common/misc/ xx(1001), delt, time
       common/pars/ ton, xmax
       common/ints/ n, nj, Numbertimesteps

       IF ( J.EQ.1 ) THEN
       DO ii = 1 , N
       DO kk = 1 , N
          B(ii,kk) = H*SME(ii,kk) - 1.5*SMP(ii,kk)
          D(ii,kk) = 2.0*SMP(ii,kk)
          X(ii,kk) = -0.5*SMP(ii,kk)
       ENDDO
          G(ii) = H*SMF(ii)
       ENDDO
       RETURN
       ENDIF
```

```
IF ( J.EQ.NJ ) THEN
DO ii = 1 , N
DO kk = 1 , N
   B(ii,kk) = H*SME(ii,kk) + 1.5*SMP(ii,kk)
   A(ii,kk) = -2.0*SMP(ii,kk)
   Y(ii,kk) = 0.5*SMP(ii,kk)
ENDDO
   G(ii) = H*SMF(ii)
ENDDO
RETURN
ENDIF
DO ii = 1 , N
DO kk = 1 , N
   A(ii,kk) = SMA(ii,kk) - H/2.0*SMB(ii,kk)
   B(ii,kk) = -2.0*SMA(ii,kk) + H**2*SMD(ii,kk)
   D(ii,kk) = SMA(ii,kk) + H/2.0*SMB(ii,kk)
ENDDO
   G(ii) = H**2*SMG(ii)
ENDDO
END

   !*******************

   SUBROUTINE BOUND_VAL(H)
   IMPLICIT NONE
   !*--BOUND_VAL225
   !*** Start of declarations inserted by SPAG
   DOUBLE PRECISION A , B , CPRev , D , D2Cdx2 , DCDx , delc , G , &
   & H , SMA , SMB , SMD , SME , SMF , SMG , SMP , X ,&
   & Y, kp,xx,delt,time,ton,xmax
   INTEGER ic , j , k , kc , N , NJ, Numbertimesteps
   !*** End of declarations inserted by SPAG
```

```
      COMMON A(15,15) , B(15,15) , DELc(15,903) , D(15,31) , G(15) , X(15,15) ,
&
      & Y(15,15)
      !COMMON /TEST / CPRev(12,903) , DCDx(12) , D2Cdx2(12)

      COMMON /SMALL / SMA(16,16) , SMB(16,16) , SMD(16,16) , SMG(16) , &
      & SME(16,16) , SMP(16,16) , SMF(16)
      COMMON /var /  CPRev(15,903) , DCDx(15) , D2Cdx2(15), kp
      common/misc/ xx(1001), delt, time
      common/pars/ ton, xmax
      common/ints/ n, nj, Numbertimesteps
      !_____________________
      ! This subroutine assumes solution of a linear boundary-value problem at
      ! a given time step. There is thus no need for iteration.
      !_____________________________
      DO j = 1 , NJ
      DO ic = 1 , N
      DO kc = 1 , N
      SMA(ic,kc) = 0.0
      SMB(ic,kc) = 0.0
      SMD(ic,kc) = 0.0
      SMP(ic,kc) = 0.0
      SME(ic,kc) = 0.0
      ENDDO
      ENDDO
      CALL FILLMAT(H,j)
      CALL ABDGXY(H,j)
      CALL BAND(j)
      ENDDO

      DO k = 1 , N
      DO j = 1 , NJ
      CPRev(k,j) = CPRev(k,j) + delc(k,j)
```

```
ENDDO
ENDDO
END

!**************************************

SUBROUTINE MATINV(N,M,Determ)
IMPLICIT NONE
!*--MATINV266
!*** Start of declarations inserted by SPAG
DOUBLE PRECISION A , B , bmax , bnext , btry , D , DELc , Determ ,&
& f , save, G,x,y
INTEGER i , id , irow , j , jc , jcol , k , M , N , nn
!*** End of declarations inserted by SPAG
DIMENSION id(15)
!!!!CHANGED HERE
COMMON A(15,15) , B(15,15) , delc(15,903) , D(15,31), G(15), X(15,15),
Y(15,15)
Determ = 1.0
DO i = 1 , N
id(i) = 0
ENDDO
DO nn = 1 , N
bmax = 1.1
DO i = 1 , N
IF ( id(i).EQ.0 ) THEN
bnext = 0.0
btry = 0.0
DO j = 1 , N
IF ( id(j).EQ.0 ) THEN
IF ( DABS(B(i,j)).GT.bnext ) THEN
bnext = DABS(B(i,j))
```

```
IF ( bnext.GT.btry ) THEN
bnext = btry
btry = DABS(B(i,j))
jc = j
ENDIF
ENDIF
ENDIF
ENDDO
IF ( bnext.LT.bmax*btry ) THEN
bmax = bnext/btry
irow = i
jcol = jc
ENDIF
ENDIF
ENDDO
IF ( id(jc).EQ.0 ) THEN
id(jcol) = 1
IF ( jcol.NE.irow ) THEN
DO j = 1 , N
save = B(irow,j)
B(irow,j) = B(jcol,j)
B(jcol,j) = save
ENDDO
DO k = 1 , M
save = D(irow,k)
D(irow,k) = D(jcol,k)
D(jcol,k) = save
ENDDO
ENDIF
f = 1.0/B(jcol,jcol)
DO j = 1 , N
B(jcol,j) = B(jcol,j)*f
ENDDO
```

```
DO k = 1 , M
D(jcol,k) = D(jcol,k)*f
ENDDO
DO i = 1 , N
IF ( i.NE.jcol ) THEN
f = B(i,jcol)
DO j = 1 , N
B(i,j) = B(i,j) - f*B(jcol,j)
ENDDO
DO k = 1 , M
D(i,k) = D(i,k) - f*D(jcol,k)
ENDDO
ENDIF
ENDDO
ELSE
Determ = 0.0
RETURN
ENDIF
ENDDO
END
!*********************************************************

SUBROUTINE BAND(J)
IMPLICIT NONE
!*--BAND345
!*** Start of declarations inserted by SPAG
DOUBLE PRECISION A , B , D , DELc , determ , e , G , X , Y
INTEGER i , J , jj , k , l , lpn , m , N , NJ , np1,Numbertimesteps
!*** End of declarations inserted by SPAG
DIMENSION e(15,16,903)
COMMON A(15,15) , B(15,15) , DELc(15,903) , D(15,31) , G(15) , X(15,15) ,
Y(15,15)
common/ints/ n, nj, Numbertimesteps
```

```
SAVE e , np1
IF ( J.LT.2 ) THEN
np1 = N + 1
DO i = 1 , N
D(i,2*N+1) = G(i)
DO l = 1 , N
lpn = l + N
D(i,lpn) = X(i,l)
ENDDO
ENDDO
CALL MATINV(N,2*N+1,determ)
IF ( determ.EQ.0 ) PRINT 99001 , J
DO k = 1 , N
e(k,np1,1) = D(k,2*N+1)
DO l = 1 , N
e(k,l,1) = -D(k,l)
lpn = l + N
X(k,l) = -D(k,lpn)
ENDDO
ENDDO
RETURN
ELSEIF ( J.EQ.2 ) THEN
DO i = 1 , N
DO k = 1 , N
DO l = 1 , N
D(i,k) = D(i,k) + A(i,l)*X(l,k)
ENDDO
ENDDO
ENDDO
ENDIF
IF ( J.GE.NJ ) THEN
DO i = 1 , N
DO l = 1 , N
```

```
G(i) = G(i) - Y(i,l)*e(l,np1,J-2)
DO m = 1 , N
A(i,l) = A(i,l) + Y(i,m)*e(m,l,J-2)
ENDDO
ENDDO
ENDDO
ENDIF
DO i = 1 , N
D(i,np1) = -G(i)
DO l = 1 , N
D(i,np1) = D(i,np1) + A(i,l)*e(l,np1,J-1)
DO k = 1 , N
B(i,k) = B(i,k) + A(i,l)*e(l,k,J-1)
ENDDO
ENDDO
ENDDO
CALL MATINV(N,np1,determ)
IF ( determ.EQ.0 ) PRINT 99001 , J
DO k = 1 , N
DO m = 1 , np1
e(k,m,J) = -D(k,m)
ENDDO
ENDDO
IF ( J.GE.NJ ) THEN
DO k = 1 , N
delc(k,J) = e(k,np1,J)
ENDDO
DO jj = 2 , NJ
m = NJ - jj + 1
DO k = 1 , N
delc(k,m) = e(k,np1,m)
DO l = 1 , N
delc(k,m) = DELc(k,m) + e(k,l,m)*delc(l,m+1)
```

```
ENDDO
ENDDO
ENDDO
DO l = 1 , N
DO k = 1 , N
delc(k,1) = delc(k,1) + X(k,l)*delc(l,3)
ENDDO
ENDDO
ENDIF
99001 FORMAT (' DETERM=0 AT J=',I4)
END
```